# Modified CRLB for Cooperative Geolocation of Two Devices Using Signals of Opportunity

Mei Leng, Wee Peng Tay, *Member, IEEE*, Chong Meng Samson See,
Sirajudeen Gulam Razul, and Moe Z. Win, *Fellow, IEEE*

***Abstract*—We consider the problem of localizing two devices using signals of opportunity from beacons with known positions. Beacons and devices have asynchronous local clocks or oscillators with unknown clock skews and offsets. We model clock skews as random, and analyze the biases introduced by clock asynchronism in the received signals. By deriving the equivalent Fisher information matrix for the modified Bayesian Cramér-Rao lower bound (CRLB) of device position and velocity estimation, we quantify the errors caused by clock asynchronism. We propose an algorithm based on differential time-difference-of-arrival (DTDOA) and frequency-difference-of-arrival (FDOA) that mitigates the effects of clock asynchronism to estimate the device positions and velocities. Simulation results suggest that our proposed algorithm is robust and approaches the CRLB when clock skews have small standard deviations.**

***Index Terms*—Asynchronous clocks, differential time-difference-of-arrival (DTDOA), localization, signals of opportunity (SOOP).**

## I. Introduction

RELIABLE, real-time and highly accurate location estimation is essential for many current and future wireless applications [1]. For example, search and rescue operations require accurate localization, and a large set of emerging wireless device network applications [2], [3] requires device locations to meaningfully interpret the collected data. A common localization method is the use of the Global Positioning System (GPS). However, GPS signals are generally limited to areas with a clear sky view, and do not penetrate well through obstacles, which makes it impractical for use in indoor and urban environments. The exploitation of signals of opportunity (SOOP) has thus been attracting much interest recently [4]–[6]. SOOP are public signals transmitted for various non-localization applications, including AM/FM radio signals [7], [8], digital television signals [9], and cellular communication signals [10]. These signals conform to well-established standards and can be easily detected in most urban areas. We call their transmitters "*beacons*" and their locations are usually known *a priori*.

Various measurements can be taken from SOOP for geolocation purposes, including received-signal-strength (RSS), angle-of-arrival (AOA), time-difference-of-arrival (TDOA) and frequency-difference-of-arrival (FDOA). Geolocation based on RSS level is a relatively cost-effective solution since the signal power function is available in most mobile devices and hence localization can be achieved without any hardware modification. However, using RSS levels for localization typically requires knowing the transmitter power and the path loss model, leading to inaccuracies if there are mismatches with the actual propagation environment. Geolocation based on AOA requires complex antenna arrays for angle measurement, which prohibits its use in smart mobile devices. Compared with the first two methods, TDOA and FDOA are attractive alternatives, since they can remove the ambiguity caused by unknown transmit time or unknown signal waveforms. This is especially important in localization using SOOP where devices usually have no such prior knowledge. Therefore, we focus on TDOA and FDOA measurements in this paper. However, the main disadvantage of this method is that at least two synchronized devices are required to cooperate with each other.

In using SOOP signals for geolocation, devices typically have no knowledge of important information like beacon transmit power, transmit time, and signal waveforms. Traditionally, a reference device with known position, called an anchor, is employed. This anchor cooperates with other devices in order to extract range measurements from the SOOP [11]. However, the maintenance of anchors can be costly, as more anchors are required to provide assistance if there are more devices spread over a larger area, or if devices are mobile. In this paper, we consider the localization of two moving devices whose locations and velocities are unknown. The solution of this problem serves as a basic building block for addressing the problem of network localization [1], where multiple devices with unknown locations and velocities cooperate to perform self-localization.

The most critical challenge for localization using SOOP is synchronization among devices and beacons [5]. In order to obtain reliable timing information, it is essential that devices and beacons are all synchronized, and therefore most existing methods make this simplifying assumption (see [10], [12] and the references therein). However, clock synchronization is difficult to achieve and maintain in practice [13], [14], and most beacons, like GSM base stations, are unaware of the presence of the devices and will not actively synchronize with them or a

Manuscript received April 2, 2013; revised September 8, 2013 and January 2, 2014; accepted March 13, 2014. Date of publication March 27, 2014; date of current version July 8, 2014. The associate editor coordinating the review of this paper and approving it for publication was A. Zajic.

M. Leng and W. P. Tay are with Nanyang Technological University, Singapore 639798 (e-mail: lengmei@ntu.edu.sg; wptay@ntu.edu.sg@ntu.edu.sg).

C. M. S. See and S. Gulam Razul are with Temasek Laboratories, Nanyang Technological University, Singapore 637553 (e-mail: samsonsee@ntu.edu.sg; ESirajudeen@ntu.edu.sg).

M. Z. Win is with the Laboratory for Information and Decision Systems, Massachusetts Institute of Technology, Cambridge, MA 02139 USA (e-mail: moewin@mit.edu).

Color versions of one or more of the figures in this paper are available online at http://ieeexplore.ieee.org.

Digital Object Identifier 10.1109/TWC.2014.2314096

common universal clock. Unlike GPS signals that are generated by satellite atomic oscillators with extremely small skews (less than $10^{-11}$, [15]), SOOP are usually generated by beacons with less perfect oscillators that have clock skews varying from $10^{-8}$ to $10^{-4}$[16], [17], which result in an accumulated clock offset up to 0.1 ms for one second. One of the main goals of this paper is to investigate how clock asynchronism affect localization and velocity estimation accuracy, and to derive fundamental limits for the estimation accuracy so as to obtain useful insights for designing practical SOOP localization methods.

Source localization algorithms using a set of asynchronous static devices were proposed in [18], where the source is assumed to emit a sequence of short pulses, and each pulse has a period that can be measured by a known number of clock ticks. A joint clock synchronization and localization algorithm for wireless sensor networks (WSNs) was proposed in [19], [20]. The major difference with our work is that anchor nodes in WSNs cooperate with sensor devices so that information such as transmit time stamp are available at the devices. In localization with SOOP, beacons are in general non-cooperative and devices do not have prior knowledge of the signal waveforms, which they cannot demodulate or decode. The reference [21] considers localization for a single device using signals from multiple synchronized beacons. However, time-of-arrival (TOA) measurements of the beacon signals are assumed to be available, which implies that the device has prior knowledge of the beacon signal. A more general case was investigated in [22] where all beacons and devices have asynchronous clocks. However, they again assume that each device can estimate the TOA of a beacon signal. In practice, the direct estimation of TOA from SOOP is difficult, since devices neither know the transmitted waveform nor are able to decode the received signal for timing information. In order to apply real-time localization, two devices must exchange their received signals and obtain local TDOA measurement by correlation [5]. The distortions from communication and local processing are therefore inevitable and are not accounted for in [21], [22].

In this paper, we investigate the localization and velocity estimation of two moving devices using arbitrary narrowband SOOP under line-of-sight (LOS) environments. We assume that the devices know the nominal carrier frequencies of the beacons but have no knowledge of their waveforms. We also assume that each device or beacon has a local oscillator that controls its clock, and we use the terms clock and oscillator interchangeably. We are interested to quantify the fundamental performance limit of device location and velocity estimation in the presence of clock asynchronism, and to develop estimation algorithms that mitigate its effects. Since the focus of this work is to quantify the effects of clock asynchronism on geolocation accuracy, we do not consider non-line-of-sight (NLOS) signals, which are of practical interest. NLOS signals present challenges that can be addressed separately [23]–[26], and are out of the scope of this paper. Our main contributions are the following:

- We analyze the biases introduced by asynchronous clocks in the beacons and devices, and derive expressions for the received signals at each device (cf. Proposition 2). We show that the time and frequency offsets in the received signals are corrupted by beacon and device clock offsets and skews. Our analysis includes the scenario studied in [22] as a special case.
- We derive the fundamental limits for device location and velocity estimation using SOOP from asynchronous beacons (cf. Theorem 1). The CRLB for localization and tracking have been extensively studied in the literature, but most works are based on the statistical characteristics of signal metrics like TDOA and FDOA [27]. As pointed out in [28], signal metrics depend heavily on the specific measurement method, which may discard useful information during processing. We treat the device clock skews as nuisance random variables, and we derive an approximate equivalent Fisher information matrix (EFIM) associated with the modified Bayesian CRLB for device locations and velocities, *directly from the received signals*. We show that the approximate EFIM does not depend on device and beacon clock offsets, which suggests that there exists estimation procedures that does not require *a priori* knowledge of these quantities.
- We propose a location estimation algorithm based on the differences between multiple TDOA estimates, which we call differential TDOA (DTDOA) [22]. Device velocities are then estimated based on the position estimates and the FDOA. Simulation results suggest that our proposed algorithm is robust to clock asychronism, and achieves a root mean squared error (RMSE) close to the CRLB when the standard deviations of device clock skews are smaller than $10^{-2}$.

The rest of this paper is organized as follows. In Section II, we present the system model. In Section III, we derive the Fisher information matrix for the modified Bayesian CRLB based on the received signals at each device. In Section IV, we obtain closed-form expressions for TDOA and FDOA estimates, and we propose an algorithm for location and velocity estimation. In Section V, we present numerical results and we conclude in Section VI. For the reader's ease of reference, we summarize some commonly used notations in Table I.

## II. System Model

We consider the problem of localizing two devices using signals from a set $\mathcal{B}$ of $N$ beacons. An example scenario is shown in Fig. 1. The beacon $b \in \mathcal{B}$ has a known fixed position $\mathbf{p}_b$, and it broadcasts a narrowband signal at a nominal carrier frequency $f_b$. Two devices, $S_1$ and $S_2$ are at unknown locations $\mathbf{p}_1$ and $\mathbf{p}_2$, and moving with unknown velocities $\mathbf{v}_1$ and $\mathbf{v}_2$, respectively. Denote the set of devices as $\mathcal{S} = \{1, 2\}$. Our goal is to estimate the locations $\mathbf{p}_j$ and velocities $\mathbf{v}_j$ for $j \in \mathcal{S}$, using SOOP from the beacons. In Section IV-C, we discuss extensions of our proposed algorithms to a network of more than two devices.

We suppose that each beacon $b$ has a local oscillator operating with clock skew $\beta_b$ and clock offset $\Omega_b$, so that its local time $t_b(t)$ with respect to a universal standard time $t$ is given by [29]

$$t_b(t) = \beta_b t + \Omega_b. \tag{1}$$

The clock skew $\beta_b$ characterizes the clock drift rate and the clock offset $\Omega_b$ characterizes any clock errors and clock drifts

TABLE I
COMMONLY USED NOTATIONS

| Notations | Definition |
|---|---|
| $\mathcal{S}$, $\mathcal{B}$ | set of devices and beacons, respectively |
| $\beta_m$, $\Omega_m$ | clock skew and clock offset of $m \in \mathcal{S} \cup \mathcal{B}$, respectively |
| $\mathcal{T}_{j,b}$, $\mathcal{D}_{j,b}$ | propagation delay and nominal Doppler shift from beacon $b$ to device $j$, respectively |
| $\mathbf{u}_{j,b}$, $\mathbf{w}_{j,b}$ | direction vectors between device $j$ and beacon $b$ defined in (3) and (27), respectively |
| $\hat{\tau}_b$, $\hat{\xi}_b$ | TDOA and FDOA estimates respectively at $S_1$ using signals of beacon $b$ |
| $\mathbf{F}_{\mathbf{x}}$ | Fisher information matrix (FIM) of the modified Bayesian CRLB for $\mathbf{x}$ |
| $\mathbf{F}_{\mathrm{e,s}}$ | equivalent Fisher information matrix (EFIM) for device location and velocity estimates |
| $\mathsf{P}_b$, $\mathsf{W}_b$, $\mathsf{T}_b$ | energy, RMS bandwidth, and RMS integration time of the signal transmitted from beacon $b$, respectively |
| $\lambda_b$, $\epsilon_b$ | contants related to beacon $b$'s signal characteristics and defined in (12) |

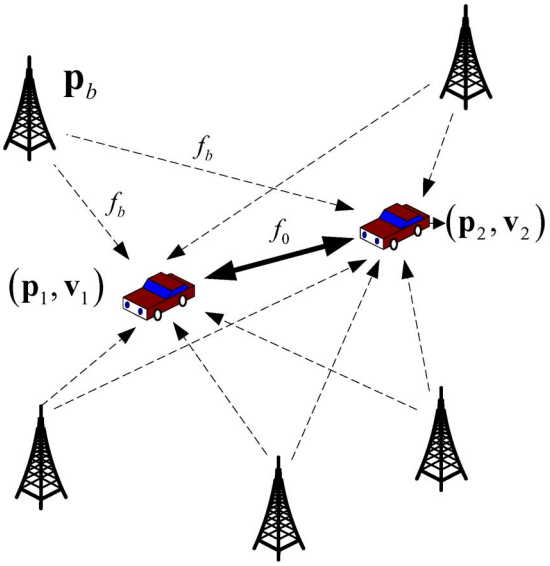


Fig. 1. Using signals from beacons to estimate device locations and velocities.

accumulated up to time $t$. We approximate the clock offset $\Omega_b$ to be constant over our observation period, and its value generally ranges from $-10$ ms to 10 ms [16]. Similarly, each device $j$ has a local oscillator with local time given by $t_j(t) = \beta_j t + \Omega_j$.

The rate at which an oscillator drifts depends on various random quantities like its quality, power level, temperature and other environmental variables. Since clock skew is non-negative, we assume that device and beacon clock skews are independent Gamma random variables with mean 1 and standard deviation $\sigma_{\beta_m}$ for $m \in \mathcal{S} \cup \mathcal{B}$. We also assume that these random variables do not depend on the beacon or device positions and velocities. The expected value of clock skews is assumed to be 1 because clocks generally drift slowly w.r.t. the standard time and its standard deviation $\sigma_{\beta_m}$ varies between $10^{-8}$ and $10^{-3}$[16], [30]. It will be obvious later that our analysis is easily generalizable to other distributions [31] as long as the quantities $\mathbb{E}\{1/\beta_m\}$ and $\mathbb{E}\{1/\beta_m^2\}$ exist and are finite.

We assume that each device has no prior knowledge of the signal waveform transmitted by beacons. However, devices know the *nominal* carrier frequencies used by the beacons and the positions of the beacons. We also assume that signals from different beacons can be distinguished at devices. Devices forward its received signals to each other by communicating over a wireless channel with nominal passband frequency $f_0$. To perform self-localization, each device obtains TDOA and FDOA measurements by cross-correlating signals received by itself and by the other device. Since local signal processing, including signal generation and sampling, depends on the local oscillator, the TDOA and FDOA measurements obtained at each device will be distorted by their asynchronous oscillators. In the following, we first analyze how such distortions affect the transmitted and received signals, and then derive closed-form expressions for TDOA and FDOA based on the distorted signals.

### A. Delays and Doppler Shifts

In this section, we briefly describe the wireless channel for communications between beacons and devices. We assume that every wireless channel has a flat fading time-varying impulse response. For each $b \in \mathcal{B}$, and each device $S_j$, $j \in \mathcal{S}$, we suppose that the channel between $b$ and $S_j$ have an impulse response $h_{j,b}(t) = \alpha_{j,b}\delta(t - \tau_{j,b}(t))$[32]. Let the propagation delay between $b$ and $S_j$ be

$$\mathcal{T}_{j,b} = \frac{\|\mathbf{p}_j - \mathbf{p}_b\|}{c} \tag{2}$$

where $c$ is the speed of light, and let the nominal Doppler shift observed at $S_j$ be

$$\mathcal{D}_{j,b} = -\frac{f_b}{c}\mathbf{v}_j^T \underbrace{\frac{\mathbf{p}_j - \mathbf{p}_b}{\|\mathbf{p}_j - \mathbf{p}_b\|}}_{\triangleq \mathbf{u}_{j,b}} \tag{3}$$

where $\mathbf{u}_{j,b}$ is the normalized direction from $S_j$ to beacon $b$. We approximate the propagation time from $b$ to $S_j$ as $\tau_{j,b}(t) \approx \mathcal{T}_{j,b} - \mathcal{D}_{j,b}t/f_b$. Similarly, we approximate the propagation time from device $S_2$ to $S_1$ as $\tau_{1,2}(t) \approx \mathcal{T}_{1,2} - \mathcal{D}_{1,2}t/f_0$, where $\mathcal{T}_{1,2} = \|\mathbf{p}_1 - \mathbf{p}_2\|/c$ and $\mathcal{D}_{1,2} = -f_0(\mathbf{v}_1 - \mathbf{v}_2)^T\mathbf{u}_{1,2}/c$ is the Doppler shift observed at $S_1$.

### B. Received Signals at Devices

Suppose that beacon $b$ generates a nominal baseband signal $g_b(t)$. Because of clock skew and offset at the beacon, the actual baseband signal is $\tilde{g}_b(t) = g_b(\beta_b t + \Omega_b)$, which is then up-converted to the nominal passband frequency $f_b$ at the beacon for transmission, and the actual passband frequency may differ from $f_b$ due to the clock skew of beacon $b$. Since we do not assume that devices know the nominal baseband signal $g_b(t)$ used by the beacon, it suffices to consider only the signal $\tilde{g}_b(t)$. However, to make the connections with TOA methods and scenarios where $g_b(t)$ is a known pilot signal clear, we have chosen to

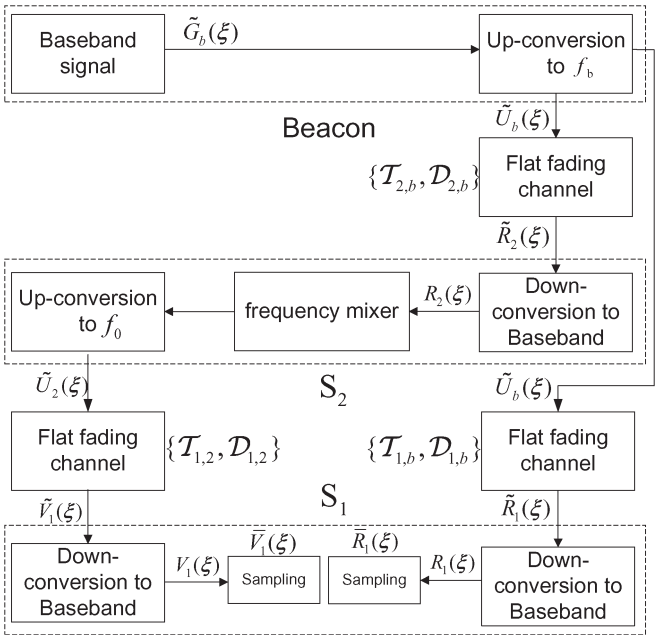


Fig. 2. Block diagram for communications between beacons and devices.

explicitly characterize signals in terms of $g_b(t)$ (cf. Remarks 1 and 2 later). Let $G_b(\xi)$ be the Fourier transform of $g_b(t)$.

The device $S_1$ receives the signal from beacon $b$, and then performs down-conversion and sampling (see Fig. 2). Each step involves signal processing using the local oscillator, which introduces errors due to its clock skew and offset. We show the signal at each processing step in Proposition 1, whose proof is straight forward, and can be found in [33]. Let $\mathrm{i} = \sqrt{-1}$, $\gamma_{1,2} = 1 + \mathcal{D}_{1,2}/f_0$, and $\gamma_{j,b} = 1 + \mathcal{D}_{j,b}/f_b$.

*Proposition 1:* Suppose that beacon $b \in \mathcal{B}$ transmits a signal with baseband representation $\tilde{G}_b(\xi)$ to device $S_j$ over a flat fading channel. We have the following.

(i) At beacon $b$, the baseband signal $\tilde{g}_b(t)$ has positive frequency part

$$\tilde{G}_b(\xi) = \frac{1}{\beta_b} G_b(\xi/\beta_b) \exp\{\mathrm{i}2\pi\xi\Omega_b/\beta_b\}.$$

(ii) At beacon $b$, the transmitted passband signal $\tilde{u}_b(t)$ has positive frequency part

$$\tilde{U}_b(\xi) = \tilde{G}_b(\xi - f_b\beta_b) \exp\{\mathrm{i}2\pi f_b\Omega_b\}.$$

(iii) At $S_j$, the passband signal received from beacon $b$, $\tilde{r}_{j,b}(t)$, has positive frequency part

$$\tilde{R}_{j,b}(\xi) = \frac{1}{\gamma_{j,b}} \tilde{U}_b(\xi/\gamma_{j,b}) \exp\{-\mathrm{i}2\pi\xi\mathcal{T}_{j,b}/\gamma_{j,b}\}.$$

(iv) At $S_j$, the signal after down conversion to baseband, $r_{j,b}(t)$, has positive frequency part

$$R_{j,b}(\xi) = \tilde{R}_{j,b}(\xi + f_b\beta_j) \exp\{-\mathrm{i}2\pi f_b\Omega_j\}.$$

(v) Suppose $S_j$ samples the received signal at Nyquist rate of $1/T$ so that the sampling impulse train is $\sum_{n=-\infty}^{+\infty} \delta(\beta_j t - nT)$. The sampled signal has positive frequency part $R_{j,b}(\beta_j\xi)$.

Device $S_1$ utilizes both its own received signal and that received by device $S_2$ to obtain TDOA and FDOA measurements. In practice, device $S_2$ forwards its received signal to $S_1$ by first doing a frequency translation to passband $f_0$ to avoid interference with all beacons, and then transmitting through the wireless channel $h_{1,2}(t) = \alpha_{1,2}\delta(\gamma_{1,2}t - \mathcal{T}_{1,2})$ (cf. Fig. 2). The received signals at device $S_1$ after sampling are given in Proposition 2, whose proof consists mainly of algebraic manipulations, and can be found in [33].

*Proposition 2:* Let $g_b(t)$ be the nominal baseband signal to be generated by beacon $b$, and $G_b(\xi)$ be its Fourier transform. The received signal at device $S_1$ from beacon $b$ has baseband representation

$$R_{1,b}(\xi) \propto G_b\left[(\beta_1\xi - \Upsilon_{1,b})/(\beta_b\gamma_{1,b})\right] \mathrm{e}^{-\mathrm{i}2\pi\xi\frac{\beta_1\Delta_{1,b}}{\beta_b\gamma_{1,b}}} \tag{4}$$

where $\Delta_{1,b} = \mathcal{T}_{1,b}\beta_b - \Omega_1\beta_b/\beta_1 - \Omega_b$ and $\Upsilon_{1,b} = f_b(\gamma_{1,b}\beta_b - \beta_1)$. The received signal at device $S_1$ from device $S_2$ has baseband representation

$$V_{1,b}(\xi) \propto G_b\left[(\beta_1\xi - \Psi_{1,b})/(\beta_b\gamma_{1,2}\gamma_{2,b})\right] \mathrm{e}^{-\mathrm{i}2\pi\xi\frac{\beta_1\Lambda_{1,b}}{\beta_b\gamma_{1,2}\gamma_{2,b}}} \tag{5}$$

where $\Lambda_{1,b} = \mathcal{T}_{2,b}\beta_b + \mathcal{T}_{1,2}\gamma_{2,b}\beta_b - \Omega_2\beta_b/\beta_2 - \Omega_b$, and $\Psi_{1,b} = f_b\gamma_{1,2}(\gamma_{2,b}\beta_b - \beta_2) + f_0(\gamma_{1,2}\beta_2 - \beta_1)$.

*Remarks 1:* Suppose that devices are static. When all beacon clocks are synchronized (i.e., $\beta_b = 1$ and $\Omega_b = 0$ for $b \in \mathcal{B}$), the received signal (4) reduces to that in [28]. Assuming further that the signal $g_b(t)$ can be generated locally by device $S_1$, the TOA estimate obtained by cross-correlating $r_{1,b}(t)$ and $g_b(t)$ is given by $\mathcal{T}_{1,b} - \Omega_1$ as in [28].

*Remarks 2:* Suppose that devices are static. The local TOA value at $S_j$ in [22] is based on time-stamp values and is given by $\mathcal{T}_{j,b}\beta_b - \Omega_1\beta_b/\beta_1 - \Omega_b$, which equals to $\Delta_{1,b}$ in Proposition 2. The TDOA between two devices $S_1$ and $S_2$ in [22] is then given by direct subtraction as $\Delta_{2,b} - \Delta_{1,b}$.

## III. Modified CRLB for Location and Velocity Estimation

In this section, we derive the fundamental limits for location and velocity estimation using the received signals at $S_1$. Let $T$ be the sampling interval, and $T_{ob}$ be the total observation time. For each beacon $b \in \mathcal{B}$, let $r_b[1 : T_{ob}/T]$ and $v_b[1 : T_{ob}/T]$ be the sampled sequence of the received signal from $b$ received at device $S_1$, and the signal from $b$ retransmitted from $S_2$ to $S_1$, respectively. Taking the inverse Fourier transform of (4) and (5), we have for each $l = 1, \ldots, T_{ob}/T$

$$r_b[l] = \underbrace{g_b(\beta_b\gamma_{1,b}lT/\beta_1 - \Delta_{1,b}) \exp\{-\mathrm{i}2\pi\Upsilon_{1,b}lT/\beta_1\}}_{\triangleq \mu_b[l]} + \varpi_b^r[l], \tag{6}$$

$$v_b[l] = \underbrace{g_b(\beta_b\gamma_{1,2}\gamma_{2,b}lT/\beta_1 - \Lambda_{1,b}) \exp\{-\mathrm{i}2\pi\Psi_{1,b}lT/\beta_1\}}_{\triangleq \theta_b[l]} + \varpi_b^v[l]. \tag{7}$$

The terms $\varpi_b^r[lt]$ and $\varpi_b^v[l]$ in (6) and (7) are additive complex white Gaussian noises with variance $\mathsf{P}_o$. Let $\mathbf{r}\{r_b[1:T_{ob}/T]: b\in\mathcal{B}\}$ and $\mathbf{v}=\{v_b[1:T_{ob}/T]: b\in\mathcal{B}\}$ be the collection of observations from all beacons.

Our analysis is based on the received sequences given by (6) and (7). Treating the device clock skews as nuisance parameters, there are $4L+2+2N$ unknown parameters $\mathbf{p}_1, \mathbf{p}_2, \mathbf{v}_1, \mathbf{v}_2, \Omega_1, \Omega_2$ and $\{\beta_b, \Omega_b\}_{b\in\mathcal{B}}$, where $L$ is the length of the position vector $\mathbf{p}_1$. We stack the unknown parameters into a vector and denote it as $\mathbf{x}=[\mathbf{p}_1^T, \mathbf{p}_2^T, \mathbf{v}_1^T, \mathbf{v}_2^T, \Omega_1, \Omega_2, \{\beta_b, \Omega_b\}_{b\in\mathcal{B}}]^T$. Let $\hat{\mathbf{x}}$ be an estimate of $\mathbf{x}$. To simplify the computations, we use the modified Bayesian CRLB [34]–[36], which allows us to first treat the device clock skews $\beta_1$ and $\beta_2$ as known values, and then taking expectation over all random clock skews. The actual Bayesian CRLB gives a tighter error bound, but has a much more complicated form that unfortunately does not provide additional insights compared to the analysis in this paper. We therefore choose to present the modified Bayesian CRLB instead. We have $\mathbb{E}\{(\hat{\mathbf{x}}-\mathbf{x})(\hat{\mathbf{x}}-\mathbf{x})^T\}\geq \mathbf{F}_{\mathbf{x}}^{-1}$, where $\mathbf{F}_{\mathbf{x}}$ is the Fisher information matrix (FIM), which can be shown to be[1]

$$\mathbf{F}_{\mathbf{x}}=\mathbb{E}_{\boldsymbol{\beta}}\left\{\mathbb{E}_{\mathbf{r},\mathbf{v}|\mathbf{x}}\left\{-\frac{\partial^2\ln p(\mathbf{r},\mathbf{v}|\mathbf{x},\beta_1,\beta_2)}{\partial\mathbf{x}\partial\mathbf{x}^T}\right\}\right\} \tag{8}$$

where $\boldsymbol{\beta}=\{\beta_m\}_{m\in\mathcal{S}\cup\mathcal{B}}$ are the random clock skews [35], [36].

### A. Equivalent Fisher Information Matrix

We map the parameter vector $\mathbf{x}$ into another parameter vector $\mathbf{y}=[\mathbf{y}_0, \mathbf{y}_1, \ldots, \mathbf{y}_N]^T$, where $\mathbf{y}_0=[\mathcal{T}_{1,2}, \mathcal{D}_{1,2}, \Omega_1, \Omega_2]$ and $\mathbf{y}_b=[\mathcal{T}_{1,b}, \mathcal{T}_{2,b}, \mathcal{D}_{1,b}, \mathcal{D}_{2,b}, \beta_b, \Omega_b]$ for $b\in\mathcal{B}$. The FIM for $\mathbf{x}$ can then be shown to be

$$\frac{\mathsf{P}_0}{2}\mathbf{F}_{\mathbf{x}}=\mathbb{E}_{\boldsymbol{\beta}}\{\mathbf{J}\mathbf{F}_{\mathbf{y}}\mathbf{J}^T\} \tag{9}$$

where $\mathbf{F}_{\mathbf{y}}$ is the FIM for $\mathbf{y}$, and $\mathbf{J}$ is the Jacobian matrix for the transformation from $\mathbf{x}$ to $\mathbf{y}$, i.e., $\mathbf{J}=\partial\mathbf{J}/\partial\mathbf{J}$. Defining matrices $\mathbf{L}_0$, $\mathbf{L}_b$, and $\{\mathbf{A}_{\{\cdot\}}, \mathbf{B}_{\{\cdot\}}, \mathbf{C}_{\{\cdot\}}, \mathbf{D}_{\{\cdot\}}\}$ in Appendix A, we obtain (10), shown at the bottom of the page, after some algebra, whose derivations can be found in Appendix A (see equation at the bottom of the page), with $\boldsymbol{\Sigma}_b=\mathbf{L}_b^T\mathbf{A}_{E,b}\mathbf{L}_b+\mathbf{L}_0^T\mathbf{A}_{H,b}\mathbf{L}_0+\mathbf{L}_0^T\mathbf{A}_{K,b}\mathbf{L}_b+\mathbf{L}_b^T\mathbf{A}_{K,b}^T\mathbf{L}_0$. Since we are interested in estimation accuracies for device locations and velocities, i.e., $\{\mathbf{p}_j, \mathbf{v}_j\}_{j=1,2}$, it is sufficient to find its equivalent Fisher information matrix (EFIM) $\mathbf{F}_{\mathrm{e,s}}$[28], [34], which is given by

$$\frac{\mathsf{P}_0}{2}\mathbf{F}_{\mathbf{e,s}}=\sum_{b\in\mathcal{B}}\mathbb{E}_{\boldsymbol{\beta}}\{\boldsymbol{\Sigma}_b\}-\mathbb{E}_{\boldsymbol{\beta}}\{\mathbf{F}_1\}\mathbb{E}_{\boldsymbol{\beta}}\{\mathbf{F}_2\}^{-1}\mathbb{E}_{\boldsymbol{\beta}}\{\mathbf{F}_1\}^T$$

where $\mathbf{F}_1$ and $\mathbf{F}_2$ represent the upper- and lower-right-corner block of $\mathbf{F}_{\mathbf{x}}$ in (10), respectively. Therefore, it follows that:

$$\frac{\mathsf{P}_0}{2}\mathbf{F}_{\mathbf{e,s}}=\sum_{b\in\mathcal{B}}\mathbf{Q}_b-\left(\sum_{b\in\mathcal{B}}\mathbf{U}_b\right)\left(\sum_{b\in\mathcal{B}}\mathbf{V}_b\right)^{-1}\left(\sum_{b\in\mathcal{B}}\mathbf{U}_b^T\right) \tag{11}$$

where

$$\begin{aligned}\mathbf{Q}_b=&\mathbf{L}_b^T\left(\bar{\mathbf{A}}_{E,b}-\bar{\mathbf{B}}_{E,b}\bar{\mathbf{D}}_{E,b}^{-1}\bar{\mathbf{B}}_{E,b}^T\right)\mathbf{L}_b\\&+\mathbf{L}_0^T\left(\bar{\mathbf{A}}_{H,b}-\bar{\mathbf{B}}_{K,b}\bar{\mathbf{D}}_{E,b}^{-1}\bar{\mathbf{B}}_{K,b}^T\right)\mathbf{L}_0\\&+\mathbf{L}_0^T\left(\bar{\mathbf{A}}_{K,b}-\bar{\mathbf{B}}_{K,b}\bar{\mathbf{D}}_{E,b}^{-1}\bar{\mathbf{B}}_{E,b}^T\right)\mathbf{L}_b\\&+\mathbf{L}_b^T\left(\bar{\mathbf{A}}_{K,b}^T-\bar{\mathbf{B}}_{E,b}\bar{\mathbf{D}}_{E,b}^{-1}\bar{\mathbf{B}}_{K,b}^T\right)\mathbf{L}_0,\\\mathbf{U}_b=&\mathbf{L}_0^T\left(\bar{\mathbf{B}}_{H,b}-\bar{\mathbf{B}}_{K,b}\bar{\mathbf{D}}_{E,b}^{-1}\bar{\mathbf{D}}_{K,b}^T\right)\\&+\mathbf{L}_b^T\left(\bar{\mathbf{C}}_{K,b}^T-\bar{\mathbf{B}}_{E,b}\bar{\mathbf{D}}_{E,b}^{-1}\bar{\mathbf{D}}_{K,b}^T\right),\\\mathbf{V}_b=&\bar{\mathbf{D}}_{H,b}-\bar{\mathbf{D}}_{K,b}\bar{\mathbf{D}}_{E,b}^{-1}\bar{\mathbf{D}}_{K,b}^T\end{aligned}$$

with $\bar{\mathbf{A}}=\mathbb{E}\boldsymbol{\beta}\mathbf{A}$ for any matrix $\mathbf{A}$.

To facilitate further analysis of the EFIM in (11), we define the signal energy $\mathsf{P}_b$, the root-mean-square (RMS) bandwidth $\mathsf{W}_b$, and the RMS integration time $\mathsf{T}_b$ for the signal $g_b(t)$ as [37]

$$\mathsf{P}_b=\int|g_b(t)|^2\,\mathrm{d}t,$$

$$\mathsf{W}_b=\left[\frac{\int|fG_b(f)|^2\,\mathrm{d}f}{\int|G_b(f)|^2\,\mathrm{d}f}\right]^{\frac{1}{2}},$$

$$\mathsf{T}_b=\left[\frac{\int|tg_b(t)|^2\,\mathrm{d}t}{\int|g_b(t)|^2\,\mathrm{d}t}\right]^{\frac{1}{2}}.$$

Without loss of generality, we assume that the signal $g_b(t)$ has zero centroid in time and frequency, hence $\mathsf{W}_b$ and $\mathsf{T}_b$

[1]The notation $\mathbb{E}_{y|x}$ means taking the expectation over $y$ conditioned on $x$, while $p(y|x)$ is the probability density function of $y$ conditioned on $x$.

$$\frac{\mathsf{P}_0}{2}\mathbf{F}_{\mathbf{x}}=\mathbb{E}_{\boldsymbol{\beta}}\left[\begin{array}{c|cccc}\sum_{b\in\mathcal{B}}\boldsymbol{\Sigma}_b & \sum_{b\in\mathcal{B}}\left(\mathbf{L}_0^T\mathbf{B}_{H,b}+\mathbf{L}_b^T\mathbf{C}_{K,b}^T\right) & \mathbf{L}_0^T\mathbf{B}_{K,1}+\mathbf{L}_1^T\mathbf{B}_{E,1} & \cdots & \mathbf{L}_0^T\mathbf{B}_{K,N}+\mathbf{L}_N^T\mathbf{B}_{E,N}\\\hline\sum_{b\in\mathcal{B}}\left(\mathbf{B}_{H,b}^T\mathbf{L}_0+\mathbf{C}_{K,b}\mathbf{L}_b\right) & \sum_{b\in\mathcal{B}}\mathbf{D}_{H,b} & \mathbf{D}_{K,1} & \cdots & \mathbf{D}_{K,N}\\\mathbf{B}_{K,1}^T\mathbf{L}_0+\mathbf{B}_{E,1}^T\mathbf{L}_1 & \mathbf{D}_{K,1}^T & \mathbf{D}_{E,1} & \cdots & \mathbf{0}\\\vdots & \vdots & \vdots & \ddots & \vdots\\\mathbf{B}_{K,N}^T\mathbf{L}_0+\mathbf{B}_{E,N}^T\mathbf{L}_N & \mathbf{D}_{K,N}^T & \mathbf{0} & \cdots & \mathbf{D}_{E,N}\end{array}\right] \tag{10}$$

characterize the signal's energy dispersion around its centroid in time and frequency, respectively. In the following, we make various assumptions and approximations, which hold in most practical applications. We use $a \ll b$ to mean that $a/b$ can be approximated by 0.

*Assumption 1:*

(i) The clock skew standard deviations $\sigma_{\beta_m} < 1$ for all $m \in \mathcal{S} \cup \mathcal{B}$.

(ii) For every beacon $b \in \mathcal{B}$, the RMS bandwidth $\mathsf{W}_b$ is much smaller than the nominal carrier frequency $f_b$ with $\mathsf{W}_b \ll f_b$.

(iii) There exists $\epsilon > 0$ and a measurable set with probability at least $1-\epsilon$ so that $\mathcal{T}_{1,2} \ll \mathsf{T}_b/3$, $\mathcal{T}_{j,b} \ll \mathsf{T}_b/3$, and $\Omega_j \ll \beta_j \mathsf{T}_b/3$, for $j = 1, 2$ and for every beacon $b \in \mathcal{B}$. Futhermore, $\epsilon$ can be chosen sufficiently small so that all expectations can be approximated by taking expectations over this set.

For each $b \in \mathcal{B}$, let $\mathsf{SNR}_n = \mathsf{P}_b/\mathsf{P}_o$ be the effective output signal-to-noise ratio of the received signal from $b$. As shown in [38], the effective output $\mathsf{SNR}_n$ depends on the input SNR and the bandwidth-time product $\mathsf{W}_b\mathsf{T}_b$. Let

$$\lambda_b = \frac{8\pi^2 \mathsf{W}_b^2 \mathsf{SNR}_b}{c^2}, \text{ and } \epsilon_b = \frac{8\pi^2 \mathsf{T}_b^2 \mathsf{SNR}_b}{c^2}. \tag{12}$$

We have the following theorem, whose proof is given in Appendix B.

*Theorem 1:* Suppose that Assumption 1 holds. Let $\boldsymbol{\phi}_b = [\mathbf{u}_{1,b}^T, -\mathbf{u}_{2,b}^T]^T$, $\boldsymbol{\phi}_s = [\mathbf{u}_{1,2}^T, -\mathbf{u}_{1,2}^T]^T$, $\boldsymbol{\rho}_b = [\mathbf{w}_{1,b}^T, -\mathbf{w}_{2,b}^T]^T$, and $\boldsymbol{\rho}_s = [\mathbf{w}_{1,2}^T, -\mathbf{w}_{1,2}^T]^T$. Treating the device clock skews as nuisance parameters, the EFIM for estimating the devices' locations and velocities at device $S_1$, denoted as $\mathbf{F}_{\mathrm{e,s}}$, is approximately given by (13), shown at the bottom of the page, where we let $\bar{\lambda}_b = \lambda_b / \sum_{b'} \lambda_{b'}$, $\sigma_s = 2[1 + (\sigma_{\beta_1}^2 - 3\sigma_{\beta_1}^2\sigma_{\beta_2}^2)/(1 - 3\sigma_{\beta_2}^2 + \sigma_{\beta_1}^2\sigma_{\beta_2}^2)]$, and

$$\boldsymbol{\Xi} = \sigma_s \sum_b \bar{\lambda}_b (\boldsymbol{\phi}_b - \boldsymbol{\phi}_s) \sum_b \bar{\lambda}_b (\boldsymbol{\phi}_b - \boldsymbol{\phi}_s)^T,$$

$$\boldsymbol{\Phi}_b = (\boldsymbol{\phi}_b - \boldsymbol{\phi}_s)(\boldsymbol{\phi}_b - \boldsymbol{\phi}_s)^T,$$

$$\mathbf{P}_b = (\boldsymbol{\rho}_b - \boldsymbol{\rho}_s)(\boldsymbol{\rho}_b - \boldsymbol{\rho}_s)^T,$$

$$\boldsymbol{\Pi}_b = (f_b\boldsymbol{\phi}_b - f_0\boldsymbol{\phi}_s)(f_b\boldsymbol{\phi}_b - f_0\boldsymbol{\phi}_s)^T,$$

$$\boldsymbol{\Gamma}_b = (\boldsymbol{\rho}_b - \boldsymbol{\rho}_s)(f_b\boldsymbol{\phi}_b - f_0\boldsymbol{\phi}_s)^T.$$

Theorem 1 provides an approximate lower bound for the location and velocity estimation errors. However, since we have used the modified Bayesian CRLB, this bound is not tight. Nevertheless, the information bound in Theorem 1 gives us various insights into the problem of location and velocity estimation, which we discuss below.

1) We see from (13) that the EFIM consists of various "information matrix" components, which we describe in the following.
   - The matrix $\boldsymbol{\Phi}_b$ can be interpreted as the ranging direction matrix (RDM) associated with the directions $\mathbf{u}_{1,b} - \mathbf{u}_{1,2}$ and $\mathbf{u}_{2,b} - \mathbf{u}_{1,2}$. This is similar to the RDM introduced in [28], where the EFIM is derived in the case where a single device localizes with the aid of synchronized anchors so that $\mathbf{u}_{1,2} = \mathbf{0}$. The RDM shows that each beacon provides only one-dimensional ranging information for each device $S_j$, along the direction $\mathbf{u}_{j,b} - \mathbf{u}_{1,2}$ with a weight $\lambda_b$ that can be interpreted as the *ranging information intensity*, which is a constant that depends only on beacon characteristics like SNR. We note that the beacon clock skews do not affect the ranging information intensity or the RDM, which is intuitively correct as TDOA ranging is not affected by beacon clock skews.
   - Let $\mathbf{u}^\perp$ be the unit vector orthogonal to $\mathbf{u}$. The vectors $\boldsymbol{\rho}_b$ and $\boldsymbol{\rho}_s$ contain Doppler shift information in the directions $\mathbf{u}_{1,b}^\perp$ and $\mathbf{u}_{1,2}^\perp$, respectively. Therefore, the matrix $\mathbf{P}_b$ can be interpreted as the relative Doppler information matrix associated with the directions $\mathbf{u}_{1,b}^\perp$, $\mathbf{u}_{2,b}^\perp$ and $\mathbf{u}_{1,2}^\perp$. This is intuitively appealing as all location information in the directions $\mathbf{u}_{1,b}$, $\mathbf{u}_{2,b}$, and $\mathbf{u}_{1,2}$ have already been captured in $\boldsymbol{\Phi}_b$ so that $\mathbf{P}_b$ contains additional information in directions orthogonal to these. Moreover, since Doppler shift is affected by beacon clock skews, we have a factor of $(1-\sigma_{\beta_b}^2)^{-1}$ multiplied to $\mathbf{P}_b$ in (13). We can also interpret $\epsilon_b$ as the *Doppler information intensity*.
   - The term $f_b\boldsymbol{\phi}_b$ is the rate of change of Doppler shift in the direction $\mathbf{u}_{j,b}$ w.r.t. $\mathbf{v}_j$. Therefore, the matrix $\boldsymbol{\Pi}_b$ contains information associated with how fast the Doppler shift along the directions $\mathbf{u}_{j,b}$ is changing w.r.t. that along $\mathbf{u}_{1,2}$. This is mainly useful for velocity estimation, and so do not appear in the CRLB derived in [12], [28]. Beacon clock skews affect the information contained in $\boldsymbol{\Pi}_b$ and appears in the multiplicative factor $(1-\sigma_{\beta_b}^2)^{-1}$ in (13).
   - The term $\boldsymbol{\Xi}$ contains the weighted average ranging information from all beacons, with the weight of beacon $b$ being $\lambda_b$ normalized by the sum of all ranging information intensities. Since $S_2$ transmits all its received signals from the beacons to $S_1$, we can interpret $\boldsymbol{\Xi}$ as the collective effect of device clock asychronism on the information transmitted from $S_2$.

$$\mathbf{F}_{\mathrm{e,s}} = \frac{1}{2} \sum_b \begin{bmatrix} \lambda_b (\boldsymbol{\Phi}_b - \boldsymbol{\Xi}) + \epsilon_b \left(1-\sigma_{\beta_b}^2\right)^{-1} \mathbf{P}_b & \epsilon_b \left(1-\sigma_{\beta_b}^2\right)^{-1} \boldsymbol{\Gamma}_b \\ \epsilon_b \left(1-\sigma_{\beta_b}^2\right)^{-1} \boldsymbol{\Gamma}_b^T & \epsilon_b \left(1-\sigma_{\beta_b}^2\right)^{-1} \boldsymbol{\Pi}_b \end{bmatrix}, \tag{13}$$

2) From (13), it is clear that the EFIM for device locations and velocities depend on neither the value of beacon clock offsets nor the value of device clocks offsets. This suggests that there exists estimation algorithms that can eliminate *both* beacon and device clock offsets. It can be shown that the TDOA procedure cancels out the beacon clock offsets. We will show in Section IV-B that the DTDOA method allows us to cancel out device clock offsets as well.
3) Although the size of clock offsets do not affect the EFIM, we observe that there is loss of information whenever device clocks are not synchronized. Consider the case where the two devices and beacons are static, so that $\boldsymbol{\rho}_b = \mathbf{0}$ and $\boldsymbol{\rho}_s = \mathbf{0}$. The EFIM in (13) for device locations reduces to

$$\mathbf{F}_{\mathrm{e},static} = \frac{1}{2}\sum_b \lambda_b(\boldsymbol{\Phi}_b - \boldsymbol{\Xi}). \tag{14}$$

On the other hand, if devices and beacons are static and synchronized, it can be shown that the EFIM is given by

$$\mathbf{F}_{\mathrm{e},syn} = \sum_b \lambda_b\left(\boldsymbol{\Phi}_b + \begin{bmatrix} \mathbf{u}_{1,b}\mathbf{u}_{1,2}^T + \mathbf{u}_{1,2}\mathbf{u}_{1,b}^T & \mathbf{u}_{1,b}(\mathbf{u}_{2,b}-\mathbf{u}_{1,2})^T \\ (\mathbf{u}_{2,b}-\mathbf{u}_{1,2})\mathbf{u}_{1,b}^T & \mathbf{0} \end{bmatrix}\right). \tag{15}$$

Therefore, the information loss due to device clock offsets is given by a non-zero quantity $\mathbf{F}_{\mathrm{e},syn} - \mathbf{F}_{\mathrm{e},static}$, and it does not depend on the value of device clock offsets, suggesting that clock offsets can be eliminated but at the price of a constant information loss.
4) As can be seen from (13), the EFIM depends on direction vectors $\mathbf{u}_{j,b}$ and $\mathbf{u}_{1,2}$ which are determined only by the relative positions of devices and beacons. To analyze the effect of beacon-device geometry on the localization performance, we consider the case (14) in two-dimensional space with static devices and beacons uniformly distributed on a circle centered at $S_1$. Letting the angle from beacon $b$ to $S_j$ be $\kappa_{j,b}$, we obtain $\mathbf{u}_{j,b} = [\cos\kappa_{j,b}, \sin\kappa_{j,b}]^T$. As the radius of the circle increases, we have in the limit of infinite radius, $\kappa_{1,b} = \kappa_{2,b}$ so that

$$\lim_{\|\mathbf{p}_b - \mathbf{p}_1\|\to\infty} \mathbf{u}_{1,b} = \lim_{\|\mathbf{p}_b - \mathbf{p}_2\|\to\infty} \mathbf{u}_{2,b} \triangleq \breve{\mathbf{u}}_b.$$

The EFIM in (14) then reduces to

$$\mathbf{F}_{\mathrm{e},static} = \sum_b \frac{\lambda_b}{2}\begin{bmatrix} \mathbf{X}_b & -\mathbf{X}_b \\ -\mathbf{X}_b & \mathbf{X}_b \end{bmatrix}$$

with $\mathbf{X}_b = (\breve{\mathbf{u}}_b + \breve{\mathbf{u}}_{1,2})(\breve{\mathbf{u}}_b + \breve{\mathbf{u}}_{1,2})^T - \sigma_s\sum_b \bar{\lambda}_b\breve{\mathbf{u}}_b\sum_b \bar{\lambda}_b\breve{\mathbf{u}}_b^T - \sigma_s\sum_b \bar{\lambda}_b\breve{\mathbf{u}}_b\mathbf{u}_{1,2}^T - \sigma_s\mathbf{u}_{1,2}\sum_b \bar{\lambda}_b\breve{\mathbf{u}}_b^T - \sigma_s\mathbf{u}_{1,2}\mathbf{u}_{1,2}^T$. It is clear that the corresponding EFIM $\mathbf{F}_{\mathrm{e},s}$ is rank-deficient, which implies that large estimation errors will be introduced when beacons are too far away from the devices. It is intuitively reasonable since the two devices appear to be a single point to a beacon when it is very far away from the devices.
5) Suppose that device $S_2$ has known location and velocity. We then have a simpler expression for the EFIM. We have $\boldsymbol{\phi}_b = \mathbf{u}_{1,b}$, $\boldsymbol{\phi}_s = \mathbf{u}_{1,2}$, $\boldsymbol{\rho}_b = \mathbf{w}_{1,b}$ and $\boldsymbol{\rho}_s = \mathbf{w}_{1,2}$, with $\boldsymbol{\Phi}_b = (\mathbf{u}_{1,b} - \mathbf{u}_{1,2})(\mathbf{u}_{1,b} - \mathbf{u}_{1,2})^T$, $\mathbf{P}_b = (\mathbf{w}_{1,b} - \mathbf{w}_{1,2})(\mathbf{w}_{1,b} - \mathbf{w}_{1,2})^T$, $\boldsymbol{\Pi}_b = (f_b\mathbf{u}_{1,b} - f_0\mathbf{u}_{1,2})(f_b\mathbf{u}_{1,b} - f_0\mathbf{u}_{1,2})^T$, and $\boldsymbol{\Gamma}_b = (\mathbf{w}_{1,b} - \mathbf{w}_{1,2})(f_b\mathbf{u}_{1,b} - f_0\mathbf{u}_{1,2})^T$. In this case, $S_2$ acts almost like an anchor, except that it does not transmit its own independent signal. Therefore, the amount of information available to $S_1$ is less than that of a true anchor.

## IV. Location and Velocity Estimation

In this section, we consider the use of TDOA and FDOA for location and velocity estimation when device and beacon clocks are not synchronized. We first evaluate the effect of clock asynchronism on TDOA and FDOA estimates, and then propose a DTDOA method to mitigate its effects.

### A. TDOA and FDOA Estimation

The TDOA and FDOA measurements between two devices are obtained by maximizing the amplitude of the complex ambiguity function $\mathcal{A}(\tau,\xi)$. At the device $S_1$, the ambiguity function w.r.t. beacon $b$ can be obtained as

$$\mathcal{A}(\tau,\xi) \propto \int V_{1,b}(f)R_{1,b}^*(f-\xi)\mathrm{e}^{\mathrm{i}2\pi f\tau}\mathrm{d}f. \tag{16}$$

Substituting (4) and (5) into (16), and maximizing $|\mathcal{A}(\tau,\xi)|$ w.r.t $\tau$ and $\xi$, the optimal solution for TDOA and FDOA estimates is then given by

$$\hat{\tau}_b \approx \beta_1\mathcal{T}_{2,b} - \beta_1\mathcal{T}_{1,b} + \beta_1\mathcal{T}_{1,2} + \Omega_1 - \frac{\beta_1}{\beta_2}\Omega_2 + e_b^\tau, \tag{17}$$

$$\hat{\xi}_b \approx \frac{\beta_b}{\beta_1}\mathcal{D}_{2,b} - \frac{\beta_b}{\beta_1}\mathcal{D}_{1,b} + \left[\frac{\beta_2}{\beta_1} + \frac{f_b}{f_0}\left(\frac{\beta_b}{\beta_1} - \frac{\beta_2}{\beta_1}\right)\right]\mathcal{D}_{1,2} + \left(1 - \frac{\beta_2}{\beta_1}\right)(f_b - f_0) + e_b^\xi, \tag{18}$$

for $b \in \mathcal{B}$, where $e_n^\tau$ and $e_n^f$ denotes estimation errors for TDOA and FDOA, respectively, and we have approximated $\gamma_{1,2} \approx 1$ and $\gamma_{j,b} \approx 1$ for $j = 1,\ 2$, since $\|\mathbf{v}_1\| \ll c$ and $\|\mathbf{v}_2\| \ll c$. In (17) and (18), the bias terms $\Omega_1 - \Omega_2\beta_1/\beta_2$ and $(1 - \beta_2/\beta_1)(f_b - f_0)$ are included in the estimated TDOA and FDOA, respectively, leading to large errors if these estimates are used directly in current TDOA and FDOA localization procedures. For example, typical crystal oscillators have a clock skew of $10^{-8}$ and can result in a bias of up to 10 ns in the TDOA estimate over a one second interval, and for every 100 MHz frequency difference between $f_b$ and $f_0$, a bias of 1 Hz will be introduced in the FDOA estimate. In the following, we propose an algorithm that eliminates these bias terms.

### *B. Location and Velocity Estimation*

Suppose there exist $N$ beacons around $S_2$ and $S_1$, a set of TDOA and FDOA estimates, $\{\hat{\tau}_b, \hat{\xi}_b\}_{b\in\mathcal{B}}$, can be obtained at each device. We in the following propose an algorithm to estimate device locations and velocities using TDOA and FDOA measurements.

*1) Location Estimation:* Let $\beta_j = 1 + \delta_{\beta_j}$ with $\delta_{\beta_j}$ being a random error such that $\mathbb{E}\{\delta_{\beta_j}\} = 0$ and $\mathbb{E}\{\delta_{\beta_j}^2\} = \sigma_{\beta_j}^2$. Substituting into (17), we have

$$c\hat{\tau}_b = \|\mathbf{p}_2 - \mathbf{p}_b\| - \|\mathbf{p}_1 - \mathbf{p}_b\| + c(\mathcal{T}_{1,2} + \Omega_1 - \Omega_2) + c\left(\delta_b^\tau + e_b^\tau\right) \tag{19}$$

where $\delta_b^\tau = \delta_{\beta_1}(\|\mathbf{p}_2 - \mathbf{p}_b\| - \|\mathbf{p}_1 - \mathbf{p}_b\| + \|\mathbf{p}_1 - \mathbf{p}_2\|)/c - \Omega_2(1+\delta_{\beta_1})/(1+\delta_{\beta_2})$. Since delay estimations from all beacons, i.e., $\{\hat{\tau}_b\}_{b\in\mathcal{B}}$, experience the same amount of biases caused by propagation delay and device clock offsets, we subtract two delay estimations and obtain

$$c(\hat{\tau}_b - \hat{\tau}_a) = \underbrace{(\|\mathbf{p}_2 - \mathbf{p}_b\| - \|\mathbf{p}_2 - \mathbf{p}_a\|) - (\|\mathbf{p}_1 - \mathbf{p}_b\| - \|\mathbf{p}_1 - \mathbf{p}_a\|)}_{\triangleq \mathbf{f}_{b,a}(\mathbf{x})} + c\left(\delta_b^\tau - \delta_a^\tau + e_b^\tau - e_a^\tau\right), \tag{20}$$

for $a \neq b$ and $\mathbf{x} = [\mathbf{p}_1^T, \mathbf{p}_2^T]^T$. We call the quantity $c(\hat{\tau}_b - \hat{\tau}_a)$ obtained in (20) the differential TDOA or DTDOA. Notice that the noise term $\delta_b^\tau - \delta_a^\tau = \delta_{\beta_1}(\|\mathbf{p}_2 - \mathbf{p}_b\| - \|\mathbf{p}_1 - \mathbf{p}_b\| - \|\mathbf{p}_2 - \mathbf{p}_a\| + \|\mathbf{p}_1 - \mathbf{p}_a\|)/c$, and it depends on the location parameters due to $\delta_{\beta_1}$. However, if $\sigma_{\beta_j}$ is small, its effect on the location estimation is negligible. Suppose there exist $N$ beacons, multiple DTDOA can be obtained for $a, b \in \{1, \ldots, N\}$. Stacking all available DTDOA into vectors, we have

$$\mathbf{z} = \mathbf{f}(\mathbf{x}) + \mathbf{e} \tag{21}$$

where $\mathbf{f}(\mathbf{x}) = [\cdots, \mathbf{f}_{b,a}(\mathbf{x}), \cdots]^T$, similarly $\mathbf{z} = [\cdots, c(\hat{\tau}_b - \hat{\tau}_a), \cdots]^T$ and $\mathbf{e} = [\cdots, c(\delta_b^\tau - \delta_a^\tau + e_b^\tau - e_a^\tau), \cdots]^T$ with covariance matrix $\mathbf{Q} = \mathbb{E}\{\mathbf{e}\mathbf{e}^T\}$. We estimate the device locations by minimizing the least square (LS) error criterion

$$(\hat{\mathbf{p}}_1, \hat{\mathbf{p}}_2) = \arg\min_{\mathbf{x}} \left(\mathbf{z} - \mathbf{f}(\mathbf{x})\right)^T \mathbf{Q}^{-1} \left(\mathbf{z} - \mathbf{f}(\mathbf{x})\right). \tag{22}$$

A closed-form solution of (22) dose not exist in general due to its non-linearity nature. Various algorithms have been investigated in the literature [18], [39]–[45]. Generally, we can linearize $\mathbf{f}(\mathbf{x})$ by a Taylor series expansion around an initial guess $\hat{\mathbf{x}}_0$ for the true parameter vector, and we have

$$\mathbf{f}(\mathbf{x}) \approx \mathbf{f}(\hat{\mathbf{x}}_0) + \mathbf{G}(\hat{\mathbf{x}}_0)(\mathbf{x} - \hat{\mathbf{x}}_0) \tag{23}$$

where $\mathbf{G}(\cdot) = [\cdots, \mathbf{G}_{b,a}^T(\cdot), \cdots]^T$ with $\mathbf{G}_{b,a}(\hat{\mathbf{x}}_0) \triangleq \nabla_{\mathbf{x}} \mathbf{f}_{b,a}(\mathbf{x})|_{\mathbf{x}=\hat{\mathbf{x}}_0}$ is the gradient of $\mathbf{f}_{b,a}(\cdot)$ evaluated at $\mathbf{x} = \hat{\mathbf{x}}_0$ and can be shown as

$$\mathbf{G}_{b,a}(\hat{\mathbf{x}}_0) = \left[ \begin{array}{c} -\frac{\mathbf{p}_1 - \mathbf{p}_b}{\|\mathbf{p}_1 - \mathbf{p}_b\|} + \frac{\mathbf{p}_1 - \mathbf{p}_a}{\|\mathbf{p}_1 - \mathbf{p}_a\|}, \\ \frac{\mathbf{p}_2 - \mathbf{p}_b}{\|\mathbf{p}_2 - \mathbf{p}_b\|} - \frac{\mathbf{p}_2 - \mathbf{p}_a}{\|\mathbf{p}_2 - \mathbf{p}_a\|} \end{array} \right]^T_{\mathbf{x}=\hat{\mathbf{x}}_0}.$$

An iterative solution of (22) by using gradient descent method is then given by

$$\hat{\mathbf{x}}^{(l+1)} = \hat{\mathbf{x}}^{(l)} + \alpha_l \left(\mathbf{G}^T\left(\hat{\mathbf{x}}^{(l)}\right)\mathbf{Q}^{-1}\mathbf{G}\left(\hat{\mathbf{x}}^{(l)}\right)\right)^{-1} \cdot \mathbf{G}^T\left(\hat{\mathbf{x}}^{(l)}\right)\mathbf{Q}^{-1}\left(\mathbf{z} - \mathbf{f}\left(\hat{\mathbf{x}}^{(l)}\right)\right), \tag{24}$$

where $\alpha_l$ is the step size in the $l$th iteration.

*2) Velocity Estimation:* We utilize FDOA estimates from all beacons, i.e., $\{\hat{\xi}_b\}_{b\in\mathcal{B}}$ to estimate the velocities of both devices. From (18) and $\beta_m = 1 + \delta_{\beta_m}$ for $m \in \mathcal{S} \cup \mathcal{B}$, we have

$$\hat{\xi}_b = \frac{f_b\hat{\mathbf{u}}_{1,b}^T - f_0\hat{\mathbf{u}}_{1,2}^T}{c}\mathbf{v}_1 - \frac{f_b\hat{\mathbf{u}}_{2,b}^T - f_0\hat{\mathbf{u}}_{1,2}^T}{c}\mathbf{v}_2 + \left(1 - \frac{\beta_2}{\beta_1}\right)(f_b - f_0) + \left(\delta_b^\xi + e_b^\xi\right), \tag{25}$$

where $\hat{\mathbf{u}}_{2,b} = (\hat{\mathbf{p}}_2 - \mathbf{p}_b)/\|\hat{\mathbf{p}}_2 - \mathbf{p}_b\|$, $\hat{\mathbf{u}}_{2,a}$, $\hat{\mathbf{u}}_{1,a}$, and $\hat{\mathbf{u}}_{1,b}$ are defined similarly, and $\delta_b^\xi = (\delta_{\beta_b} - \delta_{\beta_1} - \delta_{\beta_b}\delta_{\beta_1})[(\hat{\mathbf{u}}_{1,b} - \hat{\mathbf{u}}_{1,2})^T\mathbf{v}_1 - (\hat{\mathbf{u}}_{2,b} - \hat{\mathbf{u}}_{1,2})^T\mathbf{v}_2]f_b/c + (\delta_{\beta_2} - \delta_{\beta_1} - \delta_{\beta_2}\delta_{\beta_1})\hat{\mathbf{u}}_{1,2}^T(\mathbf{v}_1 - \mathbf{v}_2)(f_b - f_0)/c$, and we have approximated $1/(1+\delta_{\beta_m}) \approx 1 - \delta_{\beta_m}$ for small $\delta_{\beta_m}$. The random variable $\delta_b^\xi$ has zero mean and depends on the velocity and the standard deviation of clock skews. When $\sigma_{\beta_m}$ is small, its effect is negligible, and we approximate $\delta_b^\xi \approx 0$. Stacking FDOA measurements from all beacons into a vector, we have

$$\underbrace{\begin{bmatrix} \hat{\xi}_1 \\ \vdots \\ \hat{\xi}_N \end{bmatrix}}_{\boldsymbol{\xi}} = \underbrace{\begin{bmatrix} \frac{(f_1\hat{\mathbf{u}}_{1,1}^T - f_0\hat{\mathbf{u}}_{1,2}^T)}{c} & -\frac{(f_1\hat{\mathbf{u}}_{2,1}^T - f_0\hat{\mathbf{u}}_{1,2}^T)}{c} & \frac{(f_1 - f_0)}{c} \\ \vdots & & \\ \frac{(f_N\hat{\mathbf{u}}_{1,N}^T - f_0\hat{\mathbf{u}}_{1,2}^T)}{c} & -\frac{(f_N\hat{\mathbf{u}}_{2,N}^T - f_0\hat{\mathbf{u}}_{1,2}^T)}{c} & \frac{(f_N - f_0)}{c} \end{bmatrix}}_{\mathbf{U}} \times \underbrace{\begin{bmatrix} \mathbf{v}_1 \\ \mathbf{v}_2 \\ \frac{c(\beta_1 - \beta_2)}{\beta_1} \end{bmatrix}}_{\mathbf{y}} + \begin{bmatrix} e_1^\xi \\ \vdots \\ e_N^\xi \end{bmatrix}. \tag{26}$$

Since the noise term in (26) has zero mean and a known variance $\mathbf{C}$, the estimates of device velocities can therefore be easily obtained by the BLUE estimator [46] and we have $\hat{\mathbf{y}} = (\mathbf{U}^T\mathbf{C}^{-1}\mathbf{U})^{-1}\mathbf{U}^T\mathbf{C}^{-1}\boldsymbol{\xi}$.

### *C. Extension to Multiple Devices*

Our localization and velocity estimation methods can be easily generalized to a network of more than two devices through the following natural extensions. We randomly choose a device, and let it broadcast its received signal from each beacon to all the other devices in the network. Each device can then perform our proposed estimation algorithms to estimate both its own location and velocity as well as the broadcasting device's location and velocity. Alternatively, a distributed procedure can be implemented in which devices exchange signals with each other only if they are within a certain range of each other. In this case, each device may have access to information from multiple neighbors, from which DTDOA and FDOA measurements can be computed. A distributed estimation procedure based on [26], [47] can then be implemented to determine all the devices' location and velocities iteratively.

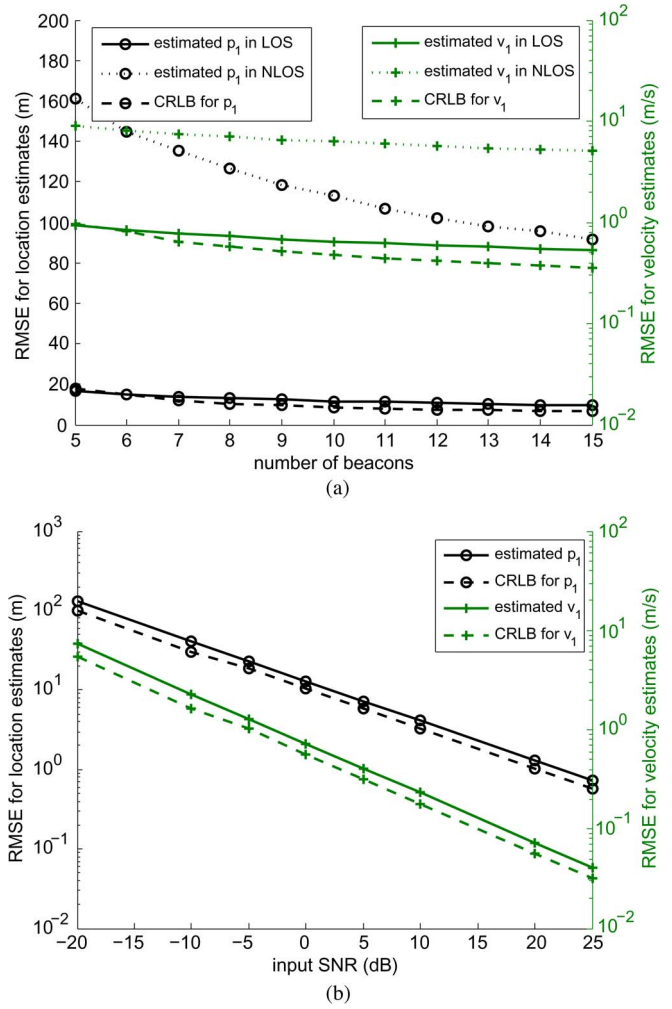


Fig. 3. Effect of measurement noise on CRLB and performance of our proposed algorithm. (a) RMSE versus $N$ with input SNR $= 0$ dB. (b) RMSE versus input SNR with $N = 8$.

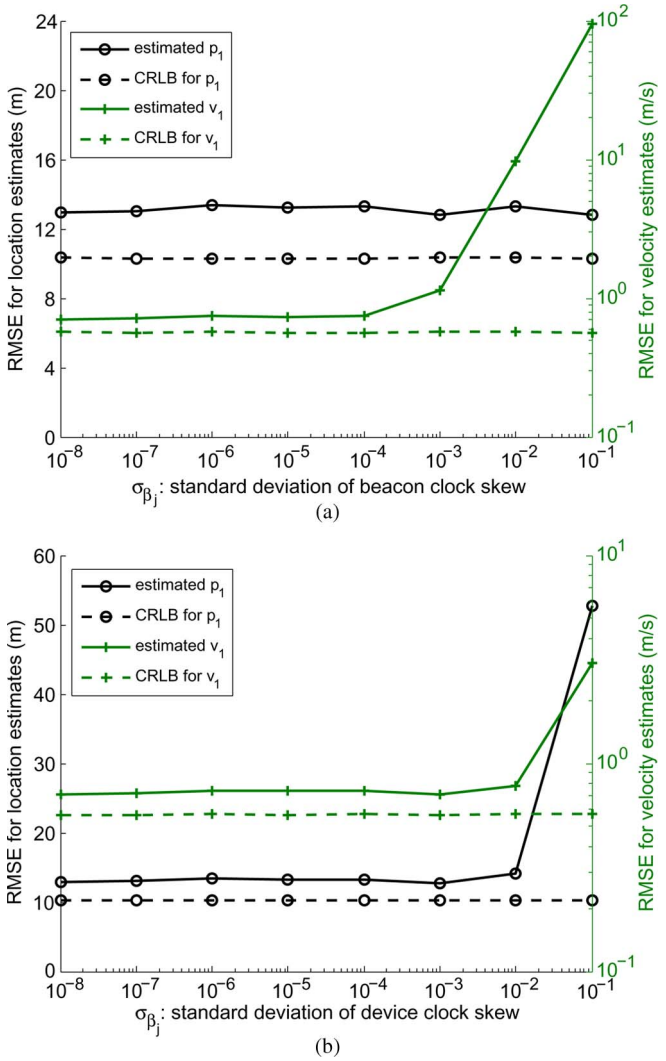


Fig. 4. Effect of clock asynchronism on CRLB and performance of our proposed algorithm. (a) Effect of beacon clock skews. (b) Effect of device clock skews.

## V. Simulation Results

Simulations are carried out to verify the CRLB and performance of our proposed algorithms. Devices $S_1$ and $S_2$ are 1 km apart, with both devices moving apart, each at a speed of 100 km/h. $N$ beacons are randomly scattered in a 10 km by 10 km area under the assumption that devices are in the convex hull of the beacons. The clock skews $\beta_m$ are drawn from Gamma distributions with $\mathbb{E}\{\beta_m\} = 1$ and varying standard deviations $\sigma_{\beta_m}$ for $m \in \mathcal{S} \cup \mathcal{B}$. The signal bandwidth is 200 kHz and the integration time is 1 s. For each set of parameters, 10 000 simulation runs are performed, a geometry of beacons is drawn randomly in each run, and the initial guess in each run is drawn randomly from the region bounded by the beacon positions.

Fig. 3 compares the performance of the proposed algorithm with the modified Bayesian CRLB under various number of beacons and measurement noise, where the standard deviations of clock skews are set to $10^{-6}$. Since approximations have been made in the algorithm and we used a looser modified CRLB, there exists a performance gap between our algorithm and the bound. When the number of beacons is larger than 8, the RMSE gap for the location and velocity estimates is almost constant at about 3.08 m and 0.17 m/s, respectively. To show the effect of multi-path channels, we conduct simulations with TDOA and FDOA estimates in the presence of NLOS errors. We follow the results in [48], and model NLOS errors as a random bias with non-zero mean within [50, 150] ns and standard deviation two times higher than that of TDOA estimated from LOS signals. The results are shown in Fig. 3(a), where it can be seen that the localization accuracy deteriorates significantly in the presence of NLOS errors. Methods to mitigate NLOS errors [23]–[26] for SOOP localization need to be investigated, and will be considered as part of our future work. Fig. 4 investigates the effect of clock asynchronism on the location and velocity estimation, where the number of beacons is set to be 8 and the input SNR is 0 dB. As shown in Figs. 4(a) and (b), the modified Bayesian CRLB is almost constant over a wide range of device and beacon clock skews, showing that clock skews have limited impact in most practical applications. The performance of the algorithm deteriorates for larger clock skews, especially for velocity estimation with varying beacon

TABLE II
EFFECT OF BIAS IN TDOA ESTIMATION

| Approach | Estimate | RMSE with $\Omega_2 = 0$ and increasing $\Omega_1$ in ns. | | | | |
|---|---|---|---|---|---|---|
| | | 0 | 5 | 50 | 100 | 200 |
| DTDOA | $\mathbf{p}_1$ (m) | 9.1855 | 9.274 | 9.278 | 9.314 | 9.355 |
| | $\mathbf{v}_1$ (m/s) | 0.453 | 0.456 | 0.455 | 0.457 | 0.462 |
| TDOA | $\mathbf{p}_1$ (m) | 7.489 | 21.315 | 199.209 | 397.657 | 792.584 |
| | $\mathbf{v}_1$ (m/s) | 0.343 | 1.160 | 11.056 | 22.026 | 43.648 |

clock skews. This is because we have approximated $\delta_b^{\xi} \approx 0$ in (25), which holds only for small $\delta_{\beta_b}$ and $\delta_{\beta_j}$. As the clock skews increase, this approximation is violated and the estimation error increases. However, we note that when the beacon clock skew is smaller than $10^{-4}$ and and the device clock skew is smaller than $10^{-2}$, our proposed algorithm achieves estimation accuracy close to the modified Bayesian CRLB. As the typical value for standard deviations of crystal oscillators ranges from $10^{-8}$ to $10^{-4}$, it is expected that our algorithm is robust in most situations.

In Table II, we compare the performance of our DTDOA approach with that of a TDOA method that uses the estimate in (17) directly without accounting for the clock offsets. We used 8 beacons surrounding the devices in a circle. It can be seen that when both device clocks have zero clock offsets, the TDOA method performs better, since the DTDOA method uses the difference between two TDOA measurements, resulting in less information being available. However, when device $S_1$'s clock offset increases, the RMSE for our DTDOA method remains relatively constant, but that for the TDOA method increases rapidly since the bias term in (17) is treated as part of the propagation delay. We see that a small clock offset can result in a significant RMSE.

## VI. CONCLUSION

In this paper, we have considered the problem of localizing two devices using signals of opportunity from beacons with known locations. We assume that all beacons and devices have free-running oscillators that have unknown clock skews and offsets. Each device performs self-localization by using TDOA and FDOA measurements between the two devices. We analyze the biases introduced by asynchronous clocks into the received signals and obtained closed-form expressions for TDOA and FDOA estimates based on these distorted signals. We derive the equivalent Fisher information matrix for the modified Bayesian CRLB using the received signal waveforms. We propose an algorithm for estimating device location and velocity based on DTDOA and FDOA estimates. Simulation results show that our algorithm is robust to clock offsets and is close to the modified Bayesian CRLB when clock skews are small.

In this paper, we have assumed for simplicity that devices forward received signals from the beacons to each other. This may be impractical or may result in high communication costs. Future research includes investigating the more practical scenario where device information exchanges are limited in bandwidth and exchange frequency. We have also limited our investigations to static beacons in this paper. The use of mobile beacons like unmanned aerial vehicles and non-GPS satellites is of practical interest.

## APPENDIX A
## DERIVATION OF $\mathbf{F_x}$ IN (10)

To derive the expression for $\mathbf{J}$, we first obtain $\partial \mathcal{T}_{1,2}/\partial \mathbf{p}_1 = \mathbf{u}_{1,2}/c$, $\partial \mathcal{D}_{1,2}/\partial \mathbf{v}_1 = -f_0 \mathbf{u}_{1,2}/c$, and

$$\frac{\partial \mathcal{D}_{1,2}}{\partial \mathbf{p}_1} = -\frac{1}{c} \underbrace{\frac{\mathbf{I} - \mathbf{u}_{1,2}\mathbf{u}_{1,2}^T}{\|\mathbf{p}_1 - \mathbf{p}_2\|}(\mathbf{v}_1 - \mathbf{v}_2) f_0}_{\triangleq \mathbf{w}_{1,2}}$$

where $\mathbf{w}_{1,2}$ is the orthogonal projection of $f_0(\mathbf{v}_1 - \mathbf{v}_2)$ onto a direction normal to $\mathbf{u}_{1,2}$. Similarly, we have $\partial \mathcal{D}_{j,b}/\partial \mathbf{v}_j = -f_b \mathbf{u}_{j,b}/c$ and

$$\frac{\partial \mathcal{D}_{j,b}}{\partial \mathbf{p}_j} = -\frac{1}{c} \underbrace{\frac{\mathbf{I} - \mathbf{u}_{j,b}\mathbf{u}_{j,b}^T}{\|\mathbf{p}_j - \mathbf{p}_b\|}\mathbf{v}_j f_b}_{\triangleq \mathbf{w}_{j,b}} \tag{27}$$

where $\mathbf{w}_{j,b}$ is orthogonal to $\mathbf{u}_{j,b}$. Utilizing these facts, it can be shown that $\mathbf{J} \in \mathbb{R}^{(4L+2+2N)\times(4+6N)}$ and $\mathbf{J} = \partial \mathbf{J}/\partial \mathbf{x} = [\mathbf{J}_0^T, \mathbf{J}_1^T, \ldots, \mathbf{J}_b^T, \ldots, \mathbf{J}_N^T]$, where

$$\mathbf{J}_0 = \left(\frac{\partial \mathbf{y}_0}{\partial \mathbf{x}}\right)^T = \left[\begin{array}{c|cc} \mathbf{L}_0 & \multicolumn{2}{c}{\mathbf{0}} \\ \hline \mathbf{0} & \mathbf{I}_2 & \mathbf{0} \end{array}\right],$$

$$\mathbf{J}_b = \left(\frac{\partial \mathbf{y}_b}{\partial \mathbf{x}}\right)^T = \left[\begin{array}{c|cc} \mathbf{L}_b & \multicolumn{2}{c}{\mathbf{0}} \\ \hline \mathbf{0} & \mathbf{0}_{2\times 2(b+1)} & \mathbf{I}_2 \quad \mathbf{0} \end{array}\right]$$

with

$$\mathbf{L}_0 = \begin{bmatrix} \frac{1}{c}\mathbf{u}_{1,2}^T & -\frac{1}{c}\mathbf{u}_{1,2}^T & \mathbf{0} & \mathbf{0} \\ -\frac{1}{c}\mathbf{w}_{1,2}^T & \frac{1}{c}\mathbf{w}_{1,2}^T & -\frac{f_0}{c}\mathbf{u}_{1,2}^T & \frac{f_0}{c}\mathbf{u}_{1,2}^T \end{bmatrix} \tag{28}$$

$$\mathbf{L}_b = \begin{bmatrix} \frac{1}{c}\mathbf{u}_{1,b}^T & \mathbf{0} & \mathbf{0} & \mathbf{0} \\ \mathbf{0} & \frac{1}{c}\mathbf{u}_{2,b}^T & \mathbf{0} & \mathbf{0} \\ -\frac{1}{c}\mathbf{w}_{1,b}^T & \mathbf{0} & -\frac{f_b}{c}\mathbf{u}_{1,b}^T & \mathbf{0} \\ \mathbf{0} & -\frac{1}{c}\mathbf{w}_{2,b}^T & \mathbf{0} & -\frac{f_b}{c}\mathbf{u}_{2,b}^T \end{bmatrix} \tag{29}$$

where $\mathbf{I}_2$ is a $2 \times 2$ identity matrix, $\mathbf{0}_{a\times b}$ is a $a \times b$ zero matrix, and the notation $\mathbf{0}$ represents a zero matrix of the appropriate dimensions, which are easily inferred from the context.

Utilizing the well known expression for the complex Gaussian CRLB [46, p.525], the matrix $\mathbf{F_y}$ can be obtained as from (8) and (9) as

$$\mathbf{F_y} = \sum_b \mathcal{R}\mathrm{e}\left\{\sum_l \frac{\partial \mu_b^*[l]}{\partial \mathbf{y}}\left(\frac{\partial \mu_b[l]}{\partial \mathbf{y}}\right)^T\right\} + \sum_b \mathcal{R}\mathrm{e}\left\{\sum_l \frac{\partial \theta_b^*[l]}{\partial \mathbf{y}}\left(\frac{\partial \theta_b[l]}{\partial \mathbf{y}}\right)^T\right\}. \tag{30}$$

Notice that $\partial \mu_b[l]/\partial \mathbf{y}_a = 0$ and $\partial \theta_b[l]/\partial \mathbf{y}_a = 0$ for all $a \neq b$, so that $\mathbf{F_y}$ is a block matrix with structure

$$\mathbf{F_y} = \left[\begin{array}{c|ccc} \sum_{b\in\mathcal{B}} \mathbf{H}_b & \mathbf{K}_1 & \cdots & \mathbf{K}_N \\ \hline \mathbf{K}_1^T & \mathbf{E}_1 & \cdots & \mathbf{0} \\ \vdots & \vdots & \ddots & \vdots \\ \mathbf{K}_N^T & \mathbf{0} & \cdots & \mathbf{E}_N \end{array}\right]$$

where

$$\mathbf{E}_b = \mathcal{R}\mathrm{e}\left\{\sum_l \frac{\partial \mu_b^*[l]}{\partial \mathbf{y}_b}\left(\frac{\partial \mu_b[l]}{\partial \mathbf{y}_b}\right)^T\right\} + \mathcal{R}\mathrm{e}\left\{\sum_l \frac{\partial \theta_b^*[l]}{\partial \mathbf{y}_b}\left(\frac{\partial \theta_b[l]}{\partial \mathbf{y}_b}\right)^T\right\},$$

$$\mathbf{H}_b = \mathcal{R}\mathrm{e}\left\{\sum_l \frac{\partial \mu_b^*[l]}{\partial \mathbf{y}_0}\left(\frac{\partial \mu_b[l]}{\partial \mathbf{y}_0}\right)^T\right\} + \mathcal{R}\mathrm{e}\left\{\sum_l \frac{\partial \theta_b^*[l]}{\partial \mathbf{y}_0}\left(\frac{\partial \theta_b[l]}{\partial \mathbf{y}_0}\right)^T\right\},$$

$$\mathbf{K}_b = \mathcal{R}\mathrm{e}\left\{\sum_l \frac{\partial \mu_b^*[l]}{\partial \mathbf{y}_0}\left(\frac{\partial \mu_b[l]}{\partial \mathbf{y}_b}\right)^T\right\} + \mathcal{R}\mathrm{e}\left\{\sum_l \frac{\partial \theta_b^*[l]}{\partial \mathbf{y}_0}\left(\frac{\partial \theta_b[l]}{\partial \mathbf{y}_b}\right)^T\right\}$$

for $b = 1, \ldots, N$. Substituting $\mathbf{J}$ and $\mathbf{F_y}$ into (9), we have

$$\frac{\mathsf{P}_0}{2}\mathbf{F}_\mathbf{x} = \sum_{b\in\mathcal{B}} \mathbb{E}_{\boldsymbol{\beta}}\left\{\mathbf{J}_0^T\mathbf{H}_b\mathbf{J}_0 + \mathbf{J}_b^T\mathbf{E}_b\mathbf{J}_b + \mathbf{J}_b^T\mathbf{K}_b^T\mathbf{J}_0 + \mathbf{J}_0^T\mathbf{K}_b\mathbf{J}_b\right\}. \tag{31}$$

To gain further insights into the structure of $\mathbf{F_x}$, we partition the matrices $\mathbf{E}_b$ such that

$$\mathbf{E}_b = \left[\begin{array}{c|c} \mathbf{A}_{E,b} & \mathbf{B}_{E,b} \\ \hline \mathbf{B}_{E,b}^T & \mathbf{D}_{E,b} \end{array}\right]$$

where $\mathbf{A}_{E,b} \in \mathbb{R}^{4\times 4}$, $\mathbf{B}_{E,b} \in \mathbb{R}^{4\times 2}$, and $\mathbf{D}_{E,b} \in \mathbb{R}^{2\times 2}$. Similarly, we have

$$\mathbf{H}_b = \left[\begin{array}{c|c} \mathbf{A}_{H,b} & \mathbf{B}_{H,b} \\ \hline \mathbf{B}_{H,b}^T & \mathbf{D}_{H,b} \end{array}\right]$$

where $\mathbf{A}_{H,b}, \mathbf{B}_{H,b}, \mathbf{D}_{H,b} \in \mathbb{R}^{2\times 2}$ and

$$\mathbf{K}_b = \left[\begin{array}{c|c} \mathbf{A}_{K,b} & \mathbf{B}_{K,b} \\ \hline \mathbf{C}_{K,b} & \mathbf{D}_{K,b} \end{array}\right]$$

where $\mathbf{A}_{K,b} \in \mathbb{R}^{2\times 4}$, $\mathbf{B}_{K,b} \in \mathbb{R}^{2\times 2}$, $\mathbf{C}_{K,b} \in \mathbb{R}^{2\times 4}$, and $\mathbf{D}_{K,b} \in \mathbb{R}^{2\times 2}$. Substituting these matrices into (31), we obtain the expression for $\mathbf{F_x}$ in (10).

## Appendix B
## Proof of Theorem 1

We first derive expressions for submatrices of $\{\mathbf{E}_b, \mathbf{H}_b, \mathbf{K}_b\}_{b=1}^N$. We summarize the results in the following Lemma 1, whose proof is given in Appendix C.

*Lemma 1:* Suppose Assumption 1 holds, the block matrix $\mathbf{V}_b$ in (11) is given by

$$\mathbf{V}_b \approx \frac{c^2\mathsf{P}_0\lambda_b}{4} \times \begin{bmatrix} 1/\left(1-\sigma_{\beta_1}^2\right) & -1/\left[\left(1-\sigma_{\beta_1}^2\right)\left(1-\sigma_{\beta_2}^2\right)\right] \\ -1/\left[\left(1-\sigma_{\beta_1}^2\right)\left(1-\sigma_{\beta_2}^2\right)\right] & \sigma_{\beta_2}^2/\left[\left(1-\sigma_{\beta_2}^2\right)^2\left(1-2\sigma_{\beta_2}^2\right)\right] \end{bmatrix}. \tag{32}$$

Suppose Assumption 1 holds, we have

$$\bar{\mathbf{A}}_{E,b} - \bar{\mathbf{B}}_{E,b}\bar{\mathbf{D}}_{E,b}^{-1}\bar{\mathbf{B}}_{E,b}^T \approx \frac{c^2\mathsf{P}_0}{4}\begin{bmatrix} \lambda_b & -\lambda_b & 0 & 0 \\ -\lambda_b & \lambda_b & 0 & 0 \\ 0 & 0 & \epsilon_b/(1-\sigma_{\beta_b}^2) & -\epsilon_b/(1-\sigma_{\beta_b}^2) \\ 0 & 0 & -\epsilon_b/(1-\sigma_{\beta_b}^2) & \epsilon_b/(1-\sigma_{\beta_b}^2) \end{bmatrix} \tag{33}$$

$$\bar{\mathbf{A}}_{H,b} - \bar{\mathbf{B}}_{K,b}\bar{\mathbf{D}}_{E,b}^{-1}\bar{\mathbf{B}}_{K,b}^T \approx \frac{c^2\mathsf{P}_0}{4}\begin{bmatrix} \lambda_b & 0 \\ 0 & \epsilon_b/(1-\sigma_{\beta_b}^2) \end{bmatrix}, \tag{34}$$

$$\bar{\mathbf{A}}_{K,b} - \bar{\mathbf{B}}_{K,b}\bar{\mathbf{D}}_{E,b}^{-1}\bar{\mathbf{B}}_{E,b}^T \approx \frac{c^2\mathsf{P}_0}{4}\begin{bmatrix} -\lambda_b & \lambda_b & 0 & 0 \\ 0 & 0 & -\epsilon_b/(1-\sigma_{\beta_b}^2) & \frac{\epsilon_b}{1-\sigma_{\beta_b}^2} \end{bmatrix}. \tag{35}$$

Next, we prove Theorem 1 using the above results. It can be seen from (11) that the EFIM for device location and velocity is given by

$$\mathbf{F}_{\mathrm{e,s}} = \frac{2}{\mathsf{P}_0}\sum_{b\in\mathcal{B}}\mathbf{Q}_b - \left(\frac{2}{c\mathsf{P}_0}\sum_{b\in\mathcal{B}}\mathbf{U}_b\right)\left(\frac{2}{c^2\mathsf{P}_0}\sum_{b\in\mathcal{B}}\mathbf{V}_b\right)^{-1}\left(\frac{2}{c\mathsf{P}_0}\sum_{b\in\mathcal{B}}\mathbf{U}_b^T\right), \tag{36}$$

which holds if and only if the matrix $\sum_b \mathbf{V}_b$ is invertible. For the first term in (36), by substituting (33)–(35) into (11), we can obtain

$$\mathbf{Q}_b = \frac{\mathsf{P}_0}{4}\begin{bmatrix} \lambda_b\boldsymbol{\Phi}_b + \epsilon_b\mathbf{P}_b/(1-\sigma_{\beta_b}^2) & \epsilon_b\boldsymbol{\Gamma}_b/(1-\sigma_{\beta_b}^2) \\ \epsilon_b\boldsymbol{\Gamma}_b^T/(1-\sigma_{\beta_b}^2) & \epsilon_b\boldsymbol{\Pi}_b/(1-\sigma_{\beta_b}^2) \end{bmatrix} \tag{37}$$

with $\boldsymbol{\Phi}_b$, $\boldsymbol{\Pi}_b$, $\mathbf{P}_b$, and $\boldsymbol{\Gamma}_b$ given in (13), where we have utilized the fact that $\mathbb{E}\{\beta_m\} = 1$ and $\mathbb{E}\{1/\beta_m\} = 1/(1-\sigma_{\beta_m}^2)$ for $m \in \mathcal{S}\cup\mathcal{B}$ when taking expectations. Similarly, it can be shown that

$$\bar{\mathbf{B}}_{H,b} - \bar{\mathbf{B}}_{K,b}\bar{\mathbf{D}}_{E,b}^{-1}\bar{\mathbf{D}}_{K,b}^T \approx \frac{c^2\mathsf{P}_0\lambda_b}{4}\begin{bmatrix} 1/(1-\sigma_{\beta_1}^2) & -1/(1-\sigma_{\beta_2}^2) \\ 0 & 0 \end{bmatrix},$$

$$\bar{\mathbf{C}}_{K,b}^T - \bar{\mathbf{B}}_{E,b}\bar{\mathbf{D}}_{E,b}^{-1}\bar{\mathbf{D}}_{K,b}^T \approx \frac{c^2\mathsf{P}_0\lambda_b}{4}\begin{bmatrix} -1/(1-\sigma_{\beta_1}^2) & 1/(1-\sigma_{\beta_2}^2) \\ 1/(1-\sigma_{\beta_1}^2) & -1/(1-\sigma_{\beta_2}^2) \\ 0 & 0 \\ 0 & 0 \end{bmatrix}.$$

Substituting these two terms into (11) and utilizing (32) and Assumption 1, we obtain

$$\left(\frac{2}{c\mathsf{P}_0}\sum_{b\in\mathcal{B}}\mathbf{U}_b\right)\left(\frac{2}{c^2\mathsf{P}_0}\sum_b\mathbf{V}_b\right)^{-1}\left(\frac{2}{c\mathsf{P}_0}\sum_{b\in\mathcal{B}}\mathbf{U}_b^T\right) \approx \sum_b\frac{\lambda_b}{2}\begin{bmatrix}\boldsymbol{\Xi} & \mathbf{0}\\ \mathbf{0} & \mathbf{0}\end{bmatrix}, \quad (38)$$

with $\boldsymbol{\Xi}$ in (13).

## Appendix C
## Proof of Lemma 1

To begin with, the expressions for $\{\mathbf{E}_b, \mathbf{H}_b, \mathbf{K}_b\}_{b=1}^N$ are derived using their definitions from (30). For the first term in (30), denoting $\boldsymbol{\eta}_\mu = [\Delta_{1,b}, \Upsilon_{1,b}]^T$ and utilizing the chain rule of derivative, we have

$$\mathcal{R}\mathrm{e}\left\{\sum_l\frac{\partial\mu_b^*[l]}{\partial\mathbf{y}_m}\left(\frac{\partial\mu_b[l]}{\partial\mathbf{y}_n}\right)^T\right\} = \frac{\partial\boldsymbol{\eta}_\mu}{\partial\mathbf{y}_m}\underbrace{\mathcal{R}\left\{\sum_l\frac{\partial\mu_b^*[l]}{\partial\boldsymbol{\eta}_\mu}\frac{\partial\mu_b[l]}{\partial\boldsymbol{\eta}_\mu^T}\right\}}_{\triangleq\mathbf{H}\mu}\frac{\partial\boldsymbol{\eta}_\mu}{\partial\mathbf{y}_n^T}, \quad (39)$$

where $m, n \in \{0, b\}$, and

$$\frac{\partial\mu_b[l]}{\partial\boldsymbol{\eta}_\mu} = \mathrm{e}^{-\mathrm{i}2\pi\Upsilon_{1,b}t/\beta_1}\begin{bmatrix}\partial g_b(\beta_b/\beta_1 t-\Delta_{1,b})/\partial\Delta_{1,b}\\ -\mathrm{i}2\pi t/\beta_1 g_b(\beta_b/\beta_1 t-\Delta_{1,b})\end{bmatrix}_{t=lT}.$$

Using definitions of $\mathsf{P}_b$, $\mathsf{T}_b$ and $\mathsf{W}_b$, it can be shown that [37]

$$\sum_l(2\pi lT)^2 g_b^*(\alpha t-\tau)\,|_{t=lT}\,g_b(\alpha t-\tau)|_{t=lT} = \frac{1}{\alpha^3}4\pi^2\mathsf{P}_b\mathsf{T}_b^2,$$

$$\sum_l\frac{\partial g_b^*(\alpha t-\tau)|_{t=lT}}{\partial\tau}\frac{\partial g_b(\alpha t-\tau)|_{t=lT}}{\partial\tau} = \frac{1}{\alpha}4\pi^2\mathsf{P}_b\mathsf{W}_b^2$$

where $T$ represents the sampling interval, and we have used the approximation of Riemann sum with $\lim_{T\to0}\sum_l g_b(lT)T \approx \int g_b(t)\mathrm{d}t$. It hence follows that:

$$\mathbf{H}_\mu = 4\pi^2\mathsf{P}_b\beta_1\begin{bmatrix}\mathsf{W}_b^2/\beta_b & 0\\ 0 & \mathsf{T}_b^2/\beta_b^3\end{bmatrix}$$

where we have assumed that $\gamma_{1,2}\approx1$ and $\gamma_{j,b}\approx1$ for $j=1$, 2. Moreover, recall that $\Delta_{1,b} = \mathcal{T}_{1,b}\beta_b - \Omega_1\beta_b/\beta_1 - \Omega_b$ and $\Upsilon_{1,b} = f_b(\gamma_{1,b}\beta_b - \beta_1)$, we have

$$\frac{\partial\boldsymbol{\eta}_\mu}{\partial\mathbf{y}_0} = \begin{bmatrix}0 & 0 & -\beta_b/\beta_1 & 0\\ 0 & 0 & 0 & 0\end{bmatrix}^T, \quad (40)$$

$$\frac{\partial\boldsymbol{\eta}_\mu}{\partial\mathbf{y}_b} = \begin{bmatrix}\beta_b & 0 & 0 & 0 & \mathcal{T}_{1,b}-\Omega_1/\beta_1 & -1\\ 0 & 0 & \beta_b & 0 & f_b\gamma_{1,b} & 0\end{bmatrix}^T. \quad (41)$$

Substituting $\mathbf{H}_\mu$, (40) and (41) into (39), we can obtain the expression for the first term in (30).

Similarly, for the second term in (30), denoting $\boldsymbol{\eta}_\theta = [\Lambda_{1,b}, \Psi_{1,b}]^T$ and utilizing the chain rule of derivative, we have

$$\mathcal{R}\mathrm{e}\left\{\sum_l\frac{\partial\theta_b^*[l]}{\partial\mathbf{y}_m}\left(\frac{\partial\theta_b[l]}{\partial\mathbf{y}_n}\right)^T\right\} = \frac{\partial\boldsymbol{\eta}_\theta}{\partial\mathbf{y}_m}\underbrace{\mathcal{R}\mathrm{e}\left\{\sum_l\frac{\partial\theta_b^*[l]}{\partial\boldsymbol{\eta}_\theta}\frac{\partial\theta_b[l]}{\partial\boldsymbol{\eta}_\theta^T}\right\}}_{\triangleq\mathbf{H}_\theta}\frac{\partial\boldsymbol{\eta}_\theta}{\partial\mathbf{y}_n^T}, \quad (42)$$

where $m, n \in \{0, b\}$. It can be shown that $\mathbf{H}_\theta = \mathbf{H}_\mu$, and recall that $\Lambda_{1,b} = \mathcal{T}_{2,b}\beta_b + \mathcal{T}_{1,2}\gamma_{2,b}\beta_b - \Omega_2\beta_b/\beta_2 - \Omega_b$ and $\Psi_{1,b} = f_b\gamma_{1,2}(\gamma_{2,b}\beta_b - \beta_2) + f_0(\gamma_{1,2}\beta_2 - \beta_1)$, we have

$$\frac{\partial\boldsymbol{\eta}_\theta}{\partial\mathbf{y}_0} = \begin{bmatrix}\gamma_{2,b}\beta_b & 0 & 0 & -\beta_b/\beta_2\\ 0 & \beta_b\gamma_{2,b}f_b/f_0+\beta_2(1-f_b/f_0) & 0 & 0\end{bmatrix}^T \quad (43)$$

$$\frac{\partial\boldsymbol{\eta}_\theta}{\partial\mathbf{y}_b} = \begin{bmatrix}0 & \beta_b & 0 & \mathcal{T}_{1,2}\beta_b/f_b & \mathcal{T}_{2,b}+\mathcal{T}_{1,2}\gamma_{2,b}-\Omega_2/\beta_2 & -1\\ 0 & 0 & 0 & \gamma_{1,2}\beta_b & f_b\gamma_{1,2}\gamma_{2,b} & 0\end{bmatrix}^T. \quad (44)$$

where $o_1 = \beta_b\gamma_{2,b}f_b/f_0 + \beta_2(1-f_b/f_0)$, and $o_2 = \mathcal{T}_{1,2}\beta_b/f_b\mathcal{T}_{2,b}\mathcal{T}_{2,b} + \mathcal{T}_{1,2}\gamma_{2,b} - \Omega_2/\beta_2$Substituting $\mathbf{H}_\theta$, (43) and (44) into (42), we can obtain the expression for the second term in (30).

Therefore, the expressions for $\{\mathbf{E}_0, \mathbf{E}_b, \mathbf{K}_b\}_{b=1}^N$ follow directly. For example

$$\mathbf{E}_b = \frac{\partial\boldsymbol{\eta}_\mu}{\partial\mathbf{y}_b}\mathbf{H}\mu\frac{\partial\boldsymbol{\eta}_\mu}{\partial\mathbf{y}_b^T} + \frac{\partial\boldsymbol{\eta}_\theta}{\partial\mathbf{y}_b}\mathbf{H}\theta\frac{\partial\boldsymbol{\eta}_\theta}{\partial\mathbf{y}_b^T}$$

substituting the results of (39)(39)–(44) into $\mathbf{E}_b$ and after some algebra, it can be shown that

$$\mathbf{D}_{E,b} \approx \frac{c^2\mathsf{P}_0\lambda_b\beta_1}{2\beta_b}\begin{bmatrix}\delta_1^2+\delta_2^2 & -(\delta_1+\delta_2)\\ -(\delta_1+\delta_2) & 2\end{bmatrix} + \frac{c^2\mathsf{P}_0\epsilon_b\beta_1}{2\beta_b^3}\begin{bmatrix}2f_b^2 & 0\\ 0 & 0\end{bmatrix}$$

where $\delta_1 = \mathcal{T}_{1,b} - \Omega_1/\beta_1$, $\delta_2 = \mathcal{T}_{2,b} + \mathcal{T}_{1,2}\gamma_{2,b} - \Omega_2/\beta_2$, and we have approximated $\gamma_{1,b} = \gamma_{2,b} = \gamma_{1,2} \approx 1$. The expression for $\bar{\mathbf{A}}_{E,b} - \bar{\mathbf{B}}_{E,b}\bar{\mathbf{D}}_{E,b}^{-1}\bar{\mathbf{B}}_{E,b}^T$ follows as:

$$\begin{aligned}&\bar{\mathbf{A}}_{E,b}-\bar{\mathbf{B}}_{E,b}\bar{\mathbf{D}}_{E,b}^{-1}\bar{\mathbf{B}}_{E,b}^T\\ &=\frac{c^2\mathsf{P}_0}{4}\mathbb{E}_{\boldsymbol{\beta}}\begin{bmatrix}\lambda_b\beta_b & -\lambda_b\beta_b & 0 & 0\\ -\lambda_b\beta_b & \lambda_b\beta_b & 0 & 0\\ 0 & 0 & \epsilon_b/\beta_b & -\epsilon_b/\beta_b\\ 0 & 0 & -\epsilon_b/\beta_b & \epsilon_b/\beta_b\end{bmatrix}\\ &\quad-\frac{c^2\mathsf{P}_0\lambda_b}{4}\mathbb{E}_{\boldsymbol{\beta}}\begin{bmatrix}\eta_1^2 & \eta_1\eta_2 & \zeta_1/f_b & \delta_1/f_b\\ \eta_1\eta_2 & \eta_2^2 & -\zeta_2/f_b & \delta_2/f_b\\ \zeta_1/f_b & -\zeta_2/f_b & -\Omega_b\zeta_1/f_b^2 & -\Omega_b\delta_1/\beta_b f_b^2\\ \delta_1/f_b & \delta_2/f_b & -\Omega_b\delta_1/\beta_b f_b^2 & 0\end{bmatrix},\end{aligned} \quad (45)$$

where $\eta_1 = \mathsf{W}_b\delta_1/(\mathsf{T}_b f_b)$, $\eta_2 = \mathsf{W}_b\delta_2/(\mathsf{T}_b f_b)$, $\zeta_1 = \Omega_b(1-\eta_1^2)/\beta_b + \delta_1$, $\zeta_2 = \Omega_b(1+\eta_1\eta_2)/\beta_b - \delta_2$. When Assumption 1 holds, we have the result in (33).

## REFERENCES


[1] M. Z. Win, A. Conti, S. Mazuelas, Y. Shen, W. M. Gifford, D. Dardari, and M. Chiani, "Network localization and navigation via cooperation," *IEEE Commun. Mag.*, vol. 49, no. 5, pp. 56–62, May 2011.

[2] W. P. Tay, J. N. Tsitsiklis, and M. Z. Win, "On the impact of node failures and unreliable communications in dense sensor networks," *IEEE Trans. Signal Process.*, vol. 56, no. 6, pp. 2535–2546, Jun. 2008.

[3] O. Kreidl and A. Willsky, "An efficient message-passing algorithm for optimizing decentralized detection networks," *IEEE Trans. Autom. Control*, vol. 55, no. 3, pp. 563–578, Mar. 2010.

[4] H. Tian, E. Mok, L. Xia, and Z. Wu, "Signals of opportunity assisted ubiquitous geolocation and navigation technology," in *Proc. SPIE*, 2008, vol. 7144, pp. 714 439-1–714 439-11.

[5] V. Moghtadaiee, S. Lim, and A. G. Dempster, "System-level considerations for signal-of-opportunity positioning," in *Proc. Int. Symp. GPS/GNSS*, Taipei, Taiwan, Oct. 2010, pp. 1–7.

[6] M. Robinson and R. Ghrist, "Topological localization via signals of opportunity," *IEEE Trans. Signal Process.*, vol. 60, no. 5, pp. 2362–2373, May 2012.

[7] S.-H. Fang, J.-C. Chen, H.-R. Huang, and T.-N. Lin, "Is FM a RF-based positioning solution in a metropolitan-scale environment? A probabilistic approach with radio measurements analysis," *IEEE Trans. Broadcast.*, vol. 55, no. 3, pp. 577–588, Sep. 2009.

[8] V. Moghtadaiee, A. G. Dempster, and S. Lim, "Indoor localization using fm radio signals: A fingerprinting approach," in *Proc. IPIN*, 2011, pp. 1–7.

[9] D. Serant, P. Thevenon, M.-L. Boucheret, O. Julien, C. Macabiau, S. Corazza, M. Dervin, and L. Ries, "Development and validation of an OFDM/DVB-T sensor for positioning," in *Proc. IEEE/ION PLANS*, 2010, pp. 988–1001.

[10] M. Bshara, U. Orguner, F. Gustafsson, and L. Van Biesen, "Robust tracking in cellular networks using hmm filters and cell-id measurements," *IEEE Trans. Veh. Technol.*, vol. 60, no. 3, pp. 1016–1024, Mar. 2011.

[11] R. K. Martin, J. S. Velotta, and J. F. Raquet, "Bandwidth efficient cooperative TDOA computation for multicarrier signals of opportunity," *IEEE Trans. Signal Process.*, vol. 57, no. 6, pp. 2311–2322, Jun. 2009.

[12] A. Yeredor and E. Angel, "Joint TDOA and FDOA estimation: A conditional bound and its use for optimally weighted localization," *IEEE Trans. Signal Process.*, vol. 59, no. 4, pp. 1612–1623, Apr. 2011.

[13] M. Leng and Y.-C. Wu, "Distributed clock synchronization for wireless sensor networks using belief propagation," *IEEE Trans. Signal Process.*, vol. 59, no. 11, pp. 5404–5414, Nov. 2011.

[14] M. Leng and Y.-C. Wu, "Low-complexity maximum-likelihood estimator for clock synchronization of wireless sensor nodes under exponential delays," *IEEE Trans. Signal Process.*, vol. 59, no. 10, pp. 4860–4870, Oct. 2011.

[15] C.-L. Cheng, F.-R. Chang, and K.-Y. Tu, "Highly accurate real-time GPS carrier phase-disciplined oscillator," *IEEE Trans. Instrum. Meas.*, vol. 54, no. 2, pp. 819–824, Apr. 2005.

[16] F. Cristian, "Probabilistic clock synchronization," *Distrib. Comput.*, vol. 3, no. 3, pp. 146–158, 1989.

[17] Hewlett-Packard Company, Fundamentals of quartz oscillators—Application note 200-2: Electronic counter series. [Online]. Available: http://literature.agilent.com/litweb/pdf/5965-7662E.pdf

[18] T. Li, A. Ekpenyong, and Y.-F. Huang, "Source localization and tracking using distributed asynchronous sensors," *IEEE Trans. Signal Process.*, vol. 54, no. 10, pp. 3991–4003, Oct. 2006.

[19] R. T. Rajan and A.-J. van der Veen, "Joint motion estimation and clock synchronization for a wireless network of mobile nodes," in *Proc. IEEE ICASSP*, 2012, pp. 2845–2848.

[20] S. P. Chepuri, R. T. Rajan, G. Leus, and A.-J. van der Veen, "Joint clock synchronization and ranging: Asymmetrical time-stamping and passive listening," *IEEE Signal Process. Lett.*, vol. 20, no. 1, pp. 51–54, Jan. 2013.

[21] M. R. Gholami, S. Gezici, and E. G. Strom, "TDOA based positioning in the presence of unknown clock skew," *IEEE Trans. Commun.*, vol. 61, no. 6, pp. 2522–2534, Jun. 2013.

[22] C. Yan and H. H. Fan, "Asynchronous differential TDOA for non-GPS navigation using signals of opportunity," in *Proc. IEEE ICASSP*, 2008, pp. 5312–5315.

[23] L. Cong and W. Zhuang, "Nonline-of-sight error mitigation in mobile location," *IEEE Trans. Wireless Commun.*, vol. 4, no. 2, pp. 560–573, Mar. 2005.

[24] I. Guvenc and C.-C. Chong, "A survey on TOA based wireless localization and NLOS mitigation techniques," *IEEE Commun. Surveys Tuts.*, vol. 11, no. 3, pp. 107–124, 3rd Quart. 2009.

[25] K. W. K. Lui, H. C. So, and W.-K. Ma, "Maximum *a posteriori* approach to time-of-arrival-based localization in non-line-of-sight environment," *IEEE Trans. Veh. Technol.*, vol. 59, no. 3, pp. 1517–1523, Mar. 2010.

[26] M. Leng, W. P. Tay, and T. Q. S. Quek, "Cooperative and distributed localization for wireless sensor networks in multipath environments," in *Proc. IEEE ICASSP*, 2012, pp. 3125–3128.

[27] H. C. So, Y. T. Chan, and F. K. W. Chan, "Closed-form formulae for time-difference-of-arrival estimation," *IEEE Trans. Signal Process.*, vol. 56, no. 6, pp. 2614–2620, Jun. 2008.

[28] Y. Shen and M. Win, "Fundamental limits of wideband localization—Part I: A general framework," *IEEE Trans. Inf. Theory*, vol. 56, no. 10, pp. 4956–4980, Oct. 2010.

[29] B. Sundararaman, U. Buy, and A. D. Kshemkalyani, "Clock synchronization for wireless sensor networks: A survey," *Ad hoc Netw. (Elsevier)*, vol. 3, no. 3, pp. 281–323, 2005.

[30] L. L. Lewis, "An introduction to frequency standards," *Proc. IEEE*, vol. 79, no. 7, pp. 927–935, Jul. 1981.

[31] D. Harris and S. Naffziger, "Statistical clock skew modeling with data delay variations," *IEEE Trans. Very Large Scale Integr. (VLSI) Syst.*, vol. 9, no. 6, pp. 888–898, Dec. 2001.

[32] R. G. Gallager, *Principles of Digital Communication*. Cambridge, U.K.: Cambridge Univ. Press, 2008.

[33] M. Leng, W. P. Tay, C. M. S. See, S. G. Razul, and M. Z. Win, Modified CRB for location and velocity estimation using signals of opportunity, arXiv:1306.0682v2 [cs.IT], Jun. 2013.

[34] K. L. B. Harry L. Van Trees, Ed., *Bayesian Bounds for Parameter Estimation and Nonlinear Filtering/Tracking*. Hoboken, NJ, USA: Wiley-IEEE, Aug. 2007.

[35] M. Moeneclaey, "On the true and the modified Cramer–Rao bounds for the estimation of a scalar parameter in the presence of nuisance parameters," *IEEE Trans. Commun.*, vol. 46, no. 11, pp. 1536–1544, Nov. 1998.

[36] F. Gini, R. Reggiannini, and U. Mengali, "The modified Cramer–Rao bound in vector parameter estimation," *IEEE Trans. Commun.*, vol. 46, no. 1, pp. 52–60, Jan. 1998.

[37] F. Hlawatsch and F. Auger, Eds., *Time-Frequency Analysis: Concepts and Methods*. Hoboken, NJ, USA: Wiley, 2008.

[38] S. Stein, "Algorithms for ambiguity function processing," *IEEE Trans. Acoust., Speech, Signal Process.*, vol. ASSP-29, no. 3, pp. 588–599, Jun. 1981.

[39] W. H. Foy, "Position-location solutions by Taylor-series estimation," *IEEE Trans. Aerosp. Electron. Syst.*, vol. AES-12, no. 2, pp. 187–194, Mar. 1976.

[40] J. Smith and J. Abel, "Closed-form least-squares source location estimation from range-difference measurements," *IEEE Trans. Acoust., Speech, Signal Process.*, vol. ASSP-35, no. 12, pp. 1661–1669, Dec. 1987.

[41] K. C. Ho and W. Xu, "An accurate algebraic solution for moving source location using TDOA and FDOA measurements," *IEEE Trans. Signal Process.*, vol. 52, no. 9, pp. 2453–2463, Sep. 2004.

[42] K. C. Ho, X. Lu, and L. Kovavisaruch, "Source localization using TDOA and FDOA measurements in the presence of receiver location errors: Analysis and solution," *IEEE Trans. Signal Process.*, vol. 55, no. 2, pp. 684–696, Feb. 2007.

[43] M. Sun and K. C. Ho, "An asymptotically efficient estimator for TDOA and FDOA positioning of multiple disjoint sources in the presence of sensor location uncertainties," *IEEE Trans. Signal Process.*, vol. 59, no. 7, pp. 3434–3440, Jul. 2011.

[44] D. Musicki, R. Kaune, and W. Koch, "Mobile emitter geolocation and tracking using TDOA and FDOA measurements," *IEEE Trans. Signal Process.*, vol. 58, no. 3, pp. 1863–1874, Mar. 2010.

[45] H.-W. Wei, R. Peng, Q. Wan, Z.-X. Chen, and S.-F. Ye, "Multidimensional scaling analysis for passive moving target localization with TDOA and FDOA measurements," *IEEE Trans. Signal Process.*, vol. 58, no. 3, pp. 1677–1688, Mar. 2010.

[46] S. M. Kay, *Fundamentals of Statistical Signal Processing: Estimation Theory*. Englewood Cliffs, NJ, USA: Prentice-Hall, 1993.

[47] N. Patwari, J. N. Ash, S. Kyperountas, A. O. H. III, R. L. Moses, and N. S. Correal, "Locating the nodes: Cooperative localization in wireless sensor networks," *IEEE Signal Process. Mag.*, vol. 22, no. 4, pp. 54–69, Jul. 2005.

[48] N. E. Gemayel, S. Koslowski, and F. K. Jondral, "A low cost tdoa localization system: Setup, challenges and results," in *Proc. 10th WPNC*, 2013, pp. 1–4.

**Mei Leng** received the B.Eng. degree from the University of Electronic Science and Technology of China, Chengdu, China, in 2005 and the Ph.D. degree from The University of Hong Kong, Pokfulam, Hong Kong, in 2011. She is currently a Research Fellow at the School of Electrical and Electronic Engineering, Nanyang Technological University, Singapore. Her current research interests include distributed algorithms, statistical signal processing and machine learning with applications to wireless sensor networks and wireless communication systems.

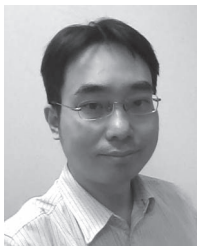

**Wee Peng Tay** (S'06–M'08) received the B.S. degree in electrical engineering and mathematics and the M.S. degree in electrical engineering from Stanford University, Stanford, CA, USA, in 2002. He received the Ph.D. degree in electrical engineering and computer science from the Massachusetts Institute of Technology, Cambridge, MA, USA, in 2008. He is currently an Assistant Professor in the School of Electrical and Electronic Engineering, Nanyang Technological University, Singapore. His research interests include distributed decision making, data fusion, distributed algorithms, communications in *ad hoc* networks, machine learning, and applied probability.

Dr. Tay received the Singapore Technologies Scholarship in 1998, the Stanford University President's Award in 1999, and the Frederick Emmons Terman Engineering Scholastic Award in 2002. He is the co-author of the Best Student Paper Award at the 46th Asilomar Conference on Signals, Systems, and Computers. He is currently serving as a Vice Chair of an Interest Group in IEEE MMTC, and has served as a Technical Program Committee member for various international conferences.

**Chong Meng Samson See** received the diploma in electronics and communications engineering (with merit) from Singapore Polytechnic, Singapore, in 1988 and both the M.Sc. degree in digital communication systems and the Ph.D. degree in electrical engineering from Loughborough University of Technology, Loughborough, U.K., in 1991 and 1999, respectively. Since 1992, he has been with DSO National Laboratories, Singapore, where he is now a Distinguished Member of the Technical Staff and is currently leading a team in the research and development of advanced array signal processing systems and algorithms. He also holds an adjunct appointment at Temasek Laboratories, Nanyang Technological University, as a Principal Research Scientist where he is Capability Manager on sensor array research. His research interests include the area of statistical and array signal processing, communications, and bio-inspired systems. He has two issued patents on direction finding. He is a Member of the IEEE and a member of the IEEE Sensor Array and Multichannel Signal Processing Technical Committee. He was Associate Editor of IEEE TRANSACTIONS ON SIGNAL PROCESSING.

**Sirajudeen Gulam Razul** received the B.Eng. and M.Eng. degrees in electrical and electronics engineering from Nanyang Technological University, Singapore, in 1997 and 2000, respectively. He received the Ph.D. degree from the University of Cambridge, Cambridge, U.K., in 2003. His Ph.D. work was on Bayesian estimation using Markov Chain Monte Carlo techniques. He was a faculty member at the School of Electrical and Electronic Engineering, Nanyang Technological University, Singapore, from 2004 to 2009. He is currently a Senior Research Scientist with Temasek Laboratories, Nanyang Technological University. His research interests include Bayesian signal processing, statistical signal processing and array processing.

**Moe Z. Win** (S'85–M'87–SM'97–F'04) received the B.S. degree (magna cum laude) in electrical engineering from Texas A&M University, College Station, TX, USA, in 1987, the M.S. degree in electrical engineering from the University of Southern California, Los Angeles, CA, USA, in 1989, and both the M.S. degree in applied mathematics and the Ph.D. degree in electrical engineering, as a Presidential Fellow, from the University of Southern California, Los Angeles, CA, USA, in 1998.

He is a Professor with the Massachusetts Institute of Technology (MIT), Cambridge, MA, USA, and founding Director of the Wireless Communication and Network Sciences Laboratory. Prior to joining MIT, he was with AT&T Research Laboratories, Middletown, NJ, USA, for five years and with the Jet Propulsion Laboratory, Pasadena, CA, USA, for seven years. His research encompasses fundamental theories, algorithm design, and experimentation for a broad range of real-world problems. His current research topics include network localization and navigation, network interference exploitation, intrinsic wireless secrecy, adaptive diversity techniques, and ultra-wide bandwidth systems.

Prof. Win is an elected Fellow of the AAAS and the IEF. He was an IEEE Distinguished Lecturer. He was honored with two IEEE Technical Field Awards: the IEEE Kiyo Tomiyasu Award in 2011 and the IEEE Eric E. Summer Award in 2006 (jointly with R. A. Scholtz). Together with students and colleagues, his papers have received numerous awards, including the IEEE Communications Society's Stephen O. Rice Prize in 2012, the IEEE Aerospace and Electronic Systems Society's M. Barry Carlton Award in 2011, the IEEE Communications Society's Guglielmo Marconi Prize Paper Award in 2008, and the IEEE Antennas and Propagation Society's Sergei A. Schelkunoff Transactions Prize Paper Award in 2003. Highlights of his international scholarly initiatives are the Copernicus Fellowship in 2009 and the Fulbright Fellowship in 2004. Other recognitions include the International Prize for Communications Cristoforo Colombo in 2013, the *Laurea Honoris Causa* from the University of Ferrara in 2008, the Technical Recognition Award of the IEEE ComSoc Radio Communications Committee in 2008, and the U.S. Presidential Early Career Award for Scientists and Engineers in 2004. He was an elected Member-at-Large on the IEEE Communications Society Board of Governors for 2011–2013. He was the Chair (2004–2006) and Secretary (2002–2004) for the Radio Communications Committee of the IEEE Communications Society. Over the last decade, he has organized and chaired numerous international conferences. He is currently Editor-at-Large for the IEEE WIRELESS COMMUNICATIONS LETTERS and is serving on the Editorial Advisory Board for IEEE TRANSACTIONS ON WIRELESS COMMUNICATIONS.